

Sponsored by –  
American Institute of Aeronautics and Astronautics (AIAA)  
Society of Automotive Engineers (SAE)

# AIAA Paper No. 72-1049

RESEARCH ON COMBUSTION INSTABILITY AND APPLICATION  
TO SOLID PROPELLANT ROCKET MOTORS, II

by  
F. E. C. CULICK  
California Institute of Technology  
Pasadena, California

# AIAA/SAE 8th Joint Propulsion Specialist Conference

NEW ORLEANS, LOUISIANA / NOVEMBER 29-DECEMBER 1, 1972

First publication rights reserved by American Institute of Aeronautics and Astronautics.  
1290 Avenue of the Americas, New York, N. Y. 10019. Abstracts may be published without  
permission if credit is given to author and to AIAA. (Price: AIAA Member \$1.50. Nonmember \$2.00).

Note: This paper available at AIAA New York office for six months;  
thereafter, photoprint copies are available at photocopy prices from  
Technical Information Service, 750 3rd Ave., New York, N. Y. 10017

-- NOTES --

# RESEARCH ON COMBUSTION INSTABILITY AND APPLICATION TO SOLID PROPELLANT ROCKET MOTORS, II\*

F. E. C. Culick\*\*

Daniel and Florence Guggenheim Jet Propulsion Center  
California Institute of Technology  
Pasadena, California

## Abstract

Unstable motions must be anticipated as a possible problem in solid-propellant rocket motors; the characteristics of an instability depend primarily on the geometry of the motor and composition of the propellant. It is the purpose of this paper to review mainly the current state of analyses of combustion instability in solid-propellant rocket motors, but appropriate measurements and observations are cited. The work discussed has become increasingly important, both for the interpretation of laboratory data and for predicting the transient behavior of disturbances in full-scale motors. Two central questions are addressed: linear stability and nonlinear behavior. Several classes of problems are discussed as special cases of a general approach to the analysis of combustion instability. Application to motors, and particularly the limitations presently understood, are stressed.

## I. Introduction

Much of Reference 1 was devoted to a review of the various gains and losses of energy which influence the behavior of small amplitude harmonic waves in a solid-propellant rocket motor. With earlier reviews, it serves as a general introduction to the topics discussed in this paper. The emphasis here is on analysis, but in the context of experimental observations and with a view to application to full-scale motors. It seems particularly important at this time to describe what analytical techniques are available and to clarify what purposes they serve.

Ultimately, the theoretical results should provide a means of predicting the stability of small disturbances and the limiting amplitude of unstable disturbances. It is not yet possible to carry out such calculations with complete satisfaction. Short of that goal, however, the framework of analysis has, in certain cases, correctly identified trends of behavior; has aided the interpretation and correlation of data; and has been used in planning experimental work. The problem of combustion instability is sufficiently complicated that experimental and analytical work must be closely coordinated if truly useful results are to be achieved. Indeed, it will probably never be possible to predict the transient characteristics of a motor totally from first principles. Certain crucial pieces of information must be obtained from independent experimental work. The most important -- and most difficult to acquire -- is the coupling between combustion and unsteady motions of the flow field.

The general problem of unsteady flow in a combustion chamber may be split into two parts:

the fluid mechanics within the volume of the chamber; and the interactions of the flow and processes at the boundary. For most purposes, it is convenient to treat the exhaust nozzle or vent as a separate problem, which is then incorporated as a boundary condition on the flow inside the chamber. Hence, the boundary consists of three pieces; inert, essentially rigid surface; burning surface; and the exhaust plane. Each of these boundaries poses its own peculiar problems. Viscous and heat transfer processes at inert surfaces can be important, both because of their influence on the flow field and for structural reasons. Although most motors using solid propellants have relatively little inert surface, at least early in a firing, this is often not true of laboratory devices such as the T-burner. Discussion of the details of these processes is minimal in this work.

On the other hand, the influences of the burning surface and the exhaust nozzle are significant in all cases. The behavior of a sonic exhaust nozzle is treated in Reference 2 and will not be covered here. In recent years, the problem of the transient characteristics of a burning surface has received a great deal of attention. Other works (References 1, 3-8) cover thoroughly both the analytical and experimental aspects; only a brief discussion is included here to summarize what is presently known and to identify current problems.

Apart from the combustion and flow problems, the dynamical behavior of the propellant may, under some circumstances, be influential. The most important effect is the dissipation of energy, but the structure and frequencies of the motions in the chamber gases may also be affected. This question too is discussed but briefly.

Thus, the concern here is almost entirely with the fluid mechanics of the unsteady flow in the chamber. There are two classes of problems to be discussed: linear stability of harmonic disturbances; and nonlinear behavior, including the growth to limiting amplitude. These are broken down further into several more restricted cases. Because much of the discussion is rather formal, it may be helpful to describe first the main approximations used and the framework for the developments in the rest of the paper.

In Section II, the formal basis for extracting special problems from the general equations of motion is given. The subject is essentially concerned with acoustics in a nonuniform average flow field with combustion. Hence, it is not surprising that the analytical problems may be classified according to the sizes of two small parameters characterizing the intensities of the steady and unsteady flow fields. The general scheme

\* This work was supported in part by the Jet Propulsion Laboratory of the California Institute of Technology; the Naval Weapons Center; Lockheed Propulsion Company; Hercules, Inc.; Aerojet Solid Propulsion Company; and Ultrasystems, Inc.

\*\* Professor of Engineering and Applied Science; Member, A. I. A. A.

outlined here produces systematically several classes of problems of varying difficulty and application. If the parameter  $\epsilon$  characterizing the unsteady field is very small, and the parameter  $\mu$  characterizing the average field is zero -- so there is no ambient flow -- then classical acoustics is recovered. But if both  $\epsilon$  and  $\mu$  are small and non-zero, and  $\epsilon/\mu \rightarrow 0$ , one obtains a system of equations widely used to study linear stability. Linear acoustics in a strong average flow field -- as in rockets with low port-to-throat ratios -- may be studied by retaining terms present for large  $\mu$ . And finally, if terms of higher order in  $\epsilon$  are retained in the equations, one may study nonlinear acoustics problems. These classes of problems are covered, roughly in order of increasing difficulty, in Sections III - VII.

Increasing interest in nonlinear aspects of combustion instability has motivated considerable coverage of the topic in this paper. The principal reason for practical interest is that the presence of unstable waves in a motor must be expected (see Reference 1, for example). The real problem is often to keep the amplitude low enough to be tolerable. Any question concerned with the amplitude of motions can be answered only by appealing to nonlinear effects.

Following the general remarks of Section II, first linear and then nonlinear problems will be discussed. A few examples of applications are included in Section X, and the work closes with a brief summary of the uncertainties and limitations of the available analyses. The coverage is necessarily brief and free of most details; some of those topics which may be less familiar are given more space. However, the main purpose is to convey the gist of what can be accomplished at the present time, and particularly what the limitations are.

It happens that so far as quantitative, a priori predictions of unsteady behavior in motors is concerned, the situation is not wholly satisfactory; but what is required to improve things is fairly clear. The formal framework provided by both the linear and nonlinear analyses is adequate to accommodate most problems of interest. Difficulties arise because some of the contributing processes cannot be specified with precision. Chief among these is the coupling between unsteady motions and surface combustion, but residual combustion and the influence of exhaust nozzles or vents are also significant. Only experimental work can provide the necessary information.

## II. Foundations for Analyses of Unsteady Motions in Combustion Chambers

One must, of course, begin with the general conservation equations. In order to account for certain important features of the flow in a solid-propellant rocket motor, the equations are written for two-phase flow. Other combustion chambers, including liquid rocket motors and thrust augmentation chambers, can be treated as special cases, but they will not be covered in this work. There are three significant assumptions used initially:

- (i) the gases are treated as a single component "average" gas having constant specific heats and obeying the perfect gas law;

- (ii) viscous forces and heat transfer within the gas are ignored;
- (iii) particulate matter is treated in an average way as a fluid.

The first strictly excludes any detailed treatment of homogeneous chemical reactions within the gas phase, but the gross effect of such reactions is represented in the usual way by including a heat source term in the energy equation written for the temperature. The second assumption is quite good for almost all problems. There are examples of weak shock waves excited in motors (Reference 9, for example); within the present analysis those must be handled in an ad hoc manner. The question will not be considered here, and all results are valid only for the smooth waveforms which are most commonly observed. The possibility of distorted, and hence steepened, waves, due to the simultaneous occurrence of several waves having different frequencies, is of course accommodated. A thorough discussion of the treatment of two-phase flows in the fashion implied by the third assumption may be found in Reference 10.

With these assumptions, the conservation equations for three-dimensional motions are

$$\text{conservation of mass (gas)} \quad \frac{\partial \rho}{\partial t} + \nabla \cdot (\rho \vec{u}) = w_p \quad (2.1)$$

$$\text{conservation of mass (particles)} \quad \frac{\partial \rho_p}{\partial t} + \nabla \cdot (\rho_p \vec{u}_p) = -w_p \quad (2.2)$$

$$\text{conservation of momentum} \quad \frac{\partial}{\partial t} (\rho \vec{u} + \rho_p \vec{u}_p) + \nabla \cdot (\rho \vec{u} \vec{u} + \rho_p \vec{u}_p \vec{u}_p) + \nabla p = 0 \quad (2.3)$$

$$\text{conservation of energy} \quad \frac{\partial}{\partial t} (\rho e_o + \rho_p e_{po}) + \nabla \cdot (\rho \vec{u} e_o + \rho_p \vec{u}_p e_{po}) + \nabla \cdot (p \vec{u}) = Q \quad (2.4)$$

The rate of conversion of solid or liquid to gas is  $w_p$  (mass/vol-sec) and  $Q$  is the rate of energy release to homogeneous chemical reactions (energy/vol-sec). For later work, it is necessary to rewrite the momentum equation and to form an equation for the pressure. One can eventually write these in the forms

$$\rho \frac{\partial \vec{u}}{\partial t} + \rho \vec{u} \cdot \nabla \vec{u} + \nabla p = \vec{F} - \vec{\sigma} \quad (2.5)$$

$$\frac{\partial p}{\partial t} + \gamma_p \nabla \cdot \vec{u} + \vec{u} \cdot \nabla p = \frac{R}{c_v} [(\vec{u}_p - \vec{u}) \cdot \vec{F} + \vec{u} \cdot \vec{\sigma} + (e_{po} - \frac{u^2}{2}) w_p + (Q + Q_p)] \quad (2.6)$$

where  $\vec{F}$  is the force of interaction between the two phases,  $Q_p$  is the heat exchanged between the two phases, and  $\vec{\sigma}$  represents a momentum exchange between the gas produced at the rate  $w_p$  and the gases already present in the chamber.

$$\vec{F} = - \left[ \rho_p \frac{\partial \vec{u}_p}{\partial t} + \rho_p \vec{u}_p \cdot \nabla \vec{u}_p \right] \quad (2.7)$$

$$Q_p = - \left[ \rho_p \frac{\partial e_p}{\partial t} + \rho_p \vec{u}_p \cdot \nabla e_p \right] \quad (2.8)$$

$$\vec{\sigma} = (\vec{u} - \vec{u}_p) w_p \quad (2.9)$$

Note that  $Q_p$  includes both energy released in combustion of solid (or liquid) and heat transfer by

conduction.

The fundamental equation used in all subsequent calculations is the nonlinear wave equation for the pressure, formed by combining (2.5) and (2.6):

$$\begin{aligned} \frac{\partial^2 p}{\partial t^2} - \frac{\gamma p}{\rho} \nabla^2 p = & \left[ \gamma_p \nabla \cdot (\vec{u} \cdot \nabla \vec{u}) - \gamma \frac{\partial p}{\partial t} \nabla \cdot \vec{u} - \frac{\partial}{\partial t} (\vec{u} \cdot \nabla p) \right] \\ & - \frac{\gamma p}{\rho} (\nabla p) \cdot (\nabla p) - \gamma_p \nabla \cdot \left( \frac{\vec{F} - \vec{\sigma}}{\rho} \right) \\ & + \frac{R}{c_v} \frac{\partial}{\partial t} \left[ (\vec{u}_p - \vec{u}) \cdot \vec{F} + \vec{u} \cdot \vec{\sigma} + \right. \\ & \left. + \left( e_{p0} - \frac{u^2}{2} \right) w_p + (Q + Q_p) \right] \quad (2.10) \end{aligned}$$

Throughout this paper,  $\gamma$  stands for the ratio  $c_p/c_v$  for the gas phase only, and  $a = (\gamma p/\rho)^{1/2}$  is the speed of sound for the gases only. The influence of the particulate matter will be computed as part of the analysis. Since eq. (2.10) also depends on the velocity field, eq. (2.5) must be solved simultaneously, both subject to suitable boundary conditions. Posed in this form, the problem is absurdly difficult without introducing further approximations. To this point, only the assumptions (i) - (iii) listed above have been used.

The approximations now introduced involve expansion of the differential equations and boundary conditions. The idea is that there are two small parameters in all problems of interest\*. These are the amplitude of the pressure disturbance (or the Mach number of the velocity disturbance) and the Mach number of the steady flow field. Let  $\epsilon$  be the measure of the amplitude of the unsteady field, i. e.,  $\epsilon \sim p'/p_0$ , and let  $\mu$  be the measure of the average Mach number. The various classes of problems treated are defined by both the absolute and relative sizes of  $\epsilon$  and  $\mu$ . If the equations (2.5) and (2.10) are solved as they stand, the results are valid for any values of  $\epsilon$  and  $\mu$ . The only available results of this general sort are numerical and have been obtained only for one-dimensional flows (see § VI).

For approximate calculations it is necessary to restrict both parameters to values less than unity. The procedure for obtaining the appropriate differential equations for the various problems is based on double expansion of the dependent variables ( $p, \rho, \vec{u}$ ) in powers of  $\epsilon$  and  $\mu$ . These are substituted in the differential equations, and one then formally examines the limit of small values, i. e.,  $\epsilon \rightarrow 0, \mu \rightarrow 0$ . In doing so, one must also specify the behavior of the ratio  $\epsilon/\mu$ . Passage to these limits is the formal means of obtaining approximate differential equations.

In accord with these remarks, one can begin by splitting all variables into the sum of mean and

\* More correctly, additional parameters may be introduced, related, for example, to the initial speed of injected liquid or to the strength of the interaction between the two phases. The two used here are the most important ones, however, and are common to all unsteady problems. More elaborate expansion schemes will not be considered at this time.

fluctuating parts:  $p = \bar{p} + p'$ , etc. The average values of course depend only on the mean flow speed, but the disturbances must be regarded as functions of both the mean flow speed (e. g. acoustic modes are distorted by nonuniform flow fields) and the amplitude of the disturbance. One way to proceed now is to expand  $\bar{p}$  in a power series in  $\mu$ , and  $p'$  in a double power series of both  $\epsilon$  and  $\mu$ ; this produces sets of linear differential equations, the combined solutions to which will provide an approximation to nonlinear behavior. However, to obtain a nonlinear problem directly,  $p'$  is expanded in series of  $\mu$  only; with the amplitude  $\epsilon$  shown explicitly, the representations used are:

$$\begin{aligned} p &= (p_0 + \mu^2 p_2 + \dots) + \epsilon (p'_0 + \mu p'_1 + \dots) \\ \vec{u} &= \vec{\mu u} + \epsilon (\vec{u}'_0 + \mu \vec{u}'_1 + \dots) \quad (2.11) \end{aligned}$$

$$\rho = (\rho_0 + \mu^2 \rho_2 + \dots) + \epsilon (\rho'_0 + \mu \rho'_1 + \dots)$$

The linear terms in  $\mu$  are of course missing in the mean pressure and density, and the mean velocity has only the linear term.

These expansions are now substituted into the differential equations, and terms of like order collected together. The terms in powers of  $\mu$  greatly complicate the calculations, and by far most of the work done has retained only the linear corrections. In § V, the linear acoustics problem for higher Mach numbers is discussed, but for the present only the linear mean flow terms will be retained. Hence, one uses

$$\begin{aligned} p &= p_0 + \epsilon p' \\ \vec{u} &= \vec{\mu u} + \epsilon \vec{u}' \\ \rho &= \rho_0 + \epsilon \rho' \end{aligned} \quad (2.12)$$

where, for simplicity,  $p'$  is now written for  $p'_0 + \mu p'_1$ , etc. After these have been used in (2.10), one can eventually write the equation in the form

$$\begin{aligned} \frac{\partial^2 p'}{\partial t^2} - a_0^2 \nabla^2 p' = & \mu \left\{ \gamma p_0 \nabla \cdot (\vec{u}' \cdot \nabla \vec{u} + \vec{u} \cdot \nabla \vec{u}') - \vec{u} \cdot \nabla \frac{\partial p'}{\partial t} - \gamma \frac{\partial p'}{\partial t} \nabla \cdot \vec{u}' \right\} \\ & + \epsilon \left\{ \gamma p_0 \nabla \cdot (\vec{u}' \cdot \nabla \vec{u}') - \gamma \frac{\partial}{\partial t} (p' \nabla \cdot \vec{u}') - \frac{\partial}{\partial t} (\vec{u}' \cdot \nabla p') \right. \\ & \left. + \gamma p_0 \nabla \cdot \left( \rho' \frac{\partial \vec{u}'}{\partial t} \right) \right\} \\ & + \frac{1}{\epsilon} \left\{ \frac{\partial P'}{\partial t} - a_0^2 \nabla \cdot (\vec{F}' - \vec{\sigma}') \right\} \quad (2.13) \end{aligned}$$

where  $P'$  is the fluctuation of

$$P = \frac{R}{c_v} \left[ (\vec{u}_p - \vec{u}) \cdot \vec{F} + \vec{u} \cdot \vec{\sigma} + \left( e_{p0} - \frac{u^2}{2} \right) w_p + (Q + Q_p) \right]. \quad (2.14)$$

It is important to emphasize that terms of order  $\epsilon^2, \mu^2, \epsilon\mu$  and higher have been consistently dropped in eq. (2.13). If the fluctuations  $P', \vec{F}',$  and  $\vec{\sigma}'$  are written out explicitly, they will simply add further terms to the brackets multiplied by  $\epsilon$  and  $\mu$ . In § V, terms of order  $\mu^2$  are retained, while the nonlinear terms in  $\epsilon$  are dropped, a

procedure which produces a set of equations valid for flows having large Mach number. Another useful case is that obtained by keeping terms of order  $\epsilon^2$ , but dropping those of order  $\mu^2$  and  $\mu\epsilon$ . This yields equations containing acoustical nonlinearities of higher order (see § VII).

If both  $\mu$  and  $\epsilon$  are zero, eq. (2.13) becomes the wave equation describing classical acoustics. But if  $\epsilon \rightarrow 0$  and the terms in  $\mu$  are retained (i. e.,  $\epsilon, \mu \rightarrow 0$  with  $\epsilon/\mu \rightarrow 0$ ), then perturbation terms of the order of the average Mach number remain. This limit is discussed in the following two sections. The complete equation is treated in § VII.

Owing to the ordering of the terms retained in this procedure, it is sufficient (indeed, required) to use, on the right hand side of (2.13), velocity and pressure fluctuations which are unperturbed by the mean flow field. This has the important consequence that it is unnecessary to solve a separate problem for the velocity field.

Then eq. (2.5) is required only to set the boundary conditions on  $p'$  for use with (2.10). The same expansion procedure applied to (2.5) leads to the condition on the normal gradient of  $p'$ :

$$\hat{n} \cdot \nabla p' = -\mu \left\{ \rho_o \frac{\partial \vec{u}'}{\partial t} \cdot \hat{n} + \rho_o (\vec{u}' \cdot \nabla \vec{u}' + \vec{u}' \cdot \nabla \vec{u}') \cdot \hat{n} \right\} - \epsilon \left\{ \rho_o \vec{u}' \cdot \nabla \vec{u}' \right\} \cdot \hat{n} + \frac{1}{\epsilon} \left\{ \vec{F}' - \vec{c}' \right\} \cdot \hat{n} \quad (2.15)$$

The first term in the first brackets contains the coupling between unsteady motions and combustion. It has therefore been shown to be of order  $\mu$ , i. e., the response of combustion is proportional to the average Mach number, based on present knowledge of the dynamical properties of a burning surface. Owing to this fact, and since terms of order  $\epsilon\mu$  have been ignored to obtain (2.15), nonlinear behavior of combustion does not appear. This is potentially a serious limitation of the approximation used here, and may eventually require that the analysis be carried out to higher order, so that terms of order  $\epsilon\mu$  at least are carried in (2.13) and (2.15).

The purpose of the preceding discussion is chiefly to outline how various approximations can be systematically constructed within one general scheme. Higher approximations can be similarly produced, but in the following four sections, only those which are currently used will be discussed.

### III. Linear One-dimensional Problems

There are two primary reasons for pursuing the one-dimensional representation: there are many practical instances of unstable motions which are closely approximated as one-dimensional flows; and the one-dimensional analysis provides approximations to essentially viscous processes, occurring in boundary layers without involving solution to the equations for viscous flows. A familiar example of this is the pressure loss computed in steady flow with mass addition at the boundary. The pressure loss is related ultimately to a dissipative and hence viscous process.

From the complete equations of motion for one-dimensional flow (see § VI), one can extract the equations for velocity and pressure corresponding to (2.5) and (2.10) above:

$$\rho S_c \frac{\partial u}{\partial t} + \rho u S_c \frac{\partial u}{\partial z} + S_c \frac{\partial p}{\partial z} = S_c (F - \sigma_1) \quad (3.1)$$

$$\frac{\partial}{\partial t} (\rho S_c) + \gamma p \frac{\partial}{\partial z} (u S_c) + u S_c \frac{\partial p}{\partial z} = (a^2 + R\Delta T_o) w + S_c P_1 \quad (3.2)$$

where

$$P_1 = \frac{R}{c_v} [(u_p - u)F + u\sigma_1 + (\epsilon_{p_o} - \frac{u^2}{2})w_p + (Q + Q_p)] \quad (3.3)$$

$$\sigma_1 = \frac{1}{S_c} [uw + u_p w^{(p)}] + (u + u_p)w_p \quad (3.4)$$

$$w = \int m_b dq \quad (3.5)$$

$$w^{(p)} = \int m_b^{(p)} dq \quad (3.6)$$

The source terms at the boundary arise from  $w$ , the rate at which gas is added per unit length of chamber, and  $w^{(p)}$ , the rate at which particulate matter is added per unit length. Thus, the first two terms of  $\sigma_1$  represent momentum exchange between the material in the chamber and that entering or leaving at the boundary.

Later calculations will show that the term  $R\Delta T_o w$  leads to a particularly interesting conclusion. By definition,  $\Delta T$  is the difference between the stagnation temperature of the gases within the chamber, and of the gases entering at the combustion zone. Hence, if the processes within the chamber are assumed to be isentropic,  $\Delta T$  represents the temperature decrement associated with nonisentropic processes. Consequently, if all processes, including the coupling between the flow and combustion, are isentropic, then  $\Delta T$  vanishes.

The expansion procedure discussed in § II, when applied to eqs. (3.1) and (3.2), leads to the nonlinear wave equation and boundary condition:

$$\begin{aligned} \frac{\partial^2 p'}{\partial t^2} - a_o^2 \frac{1}{S_c} \frac{\partial}{\partial z} \left( S_c \frac{\partial p'}{\partial z} \right) = & \mu \left\{ \gamma_{p_o} \frac{1}{S_c} \frac{\partial}{\partial z} \left( S_c \frac{\partial}{\partial z} (\overline{uu'}) \right) \right. \\ & \left. - \overline{u} \frac{\partial^2 p'}{\partial z \partial t} - \frac{\gamma}{S_c} \frac{\partial p'}{\partial t} \frac{d}{dz} (\overline{uS_c}) \right\} \\ + \epsilon \left\{ \gamma_{p_o} \frac{1}{S_c} \frac{\partial}{\partial z} \left( S_c u' \frac{\partial u'}{\partial z} \right) - \frac{\gamma}{S_c} \frac{\partial}{\partial t} \left( p' \frac{\partial}{\partial z} (S_c u') \right) \right. \\ & \left. - \frac{\partial}{\partial t} \left( u' \frac{\partial p'}{\partial z} \right) + \frac{\gamma p_o}{S_c} \frac{\partial}{\partial z} \left( S_c p' \frac{\partial u'}{\partial t} \right) \right\} \\ + \frac{1}{\epsilon} \left\{ \frac{\partial P_1}{\partial t} - \frac{a_o^2}{S_c} \frac{\partial}{\partial z} [S_c (F' - \sigma_1')] \right. \\ & \left. + \frac{1}{S_c} \frac{\partial}{\partial z} [(a^2 + R\Delta T_o)w] \right\} \quad (3.7) \end{aligned}$$

$$\frac{\partial p'}{\partial z} = -\mu \left\{ \rho_o \frac{\partial u'}{\partial t} + \rho_o \frac{\partial}{\partial z} (\overline{uu'}) \right\} - \epsilon \left\{ \rho_o u' \frac{\partial u'}{\partial t} \right\} + \frac{1}{\epsilon} (F' - \sigma_1') \quad (3.8)$$

The boundary condition is of course applied at  $z = 0$  and  $z = L$ .

For linear problems, the bracket multiplied by  $\epsilon$  is dropped ( $\epsilon \rightarrow 0$ ). The equation can be solved formally for arbitrary motions, but it is

usually adequate for practical purposes to consider only harmonic motions. The results then can be used to answer the question: will an initially small disturbance grow or decay? This problem, of linear stability, is based on using the time dependence  $\exp(ia_0 kt)$  for all fluctuations. The complex wavenumber is  $k$ , of which the real part gives the angular frequency and the imaginary part provides the growth or decay constant  $\alpha$ :  $a_0 k = \omega - i\alpha$ . In order that all disturbances be linearly stable,  $\alpha$  must be negative.

With the assumed harmonic time dependence,  $p' = \hat{p} \exp(ia_0 kt)$ , the inhomogeneous wave equation to be solved is

$$\frac{1}{S_c} \frac{d}{dz} \left( S_c \frac{d\hat{p}}{dz} \right) + k^2 \hat{p} = \hat{h}_1 \quad (3.8)$$

subject to the boundary condition

$$\frac{d\hat{p}}{dz} = -\hat{f}_1 \quad (z = 0, L) \quad (3.9)$$

where

$$\begin{aligned} \hat{h}_1 = & -\rho_0 \frac{d^2}{dz^2} (\bar{u}\hat{u}) + \frac{1}{S_c} \frac{d}{dz} [S_c (\hat{F} - \hat{\sigma}_1)] + ik \frac{\bar{u}}{a_0} \frac{d\hat{p}}{dz} \\ & + ik \frac{\bar{v}}{2} \hat{p} \frac{1}{S_c} \frac{d}{dz} (\bar{u}S_c) - \rho_0 \frac{\partial}{\partial z} (\bar{u}\hat{u}) - \frac{d \ln S_c}{dz} - \frac{ik}{a_0} \hat{p}_1 \end{aligned} \quad (3.10)$$

$$\hat{f}_1 = ik\rho_0 \hat{u} + ik\rho_0 \bar{u}\hat{u} - (\hat{F} - \hat{\sigma}_1) \quad (3.11)$$

The ordering parameter  $\mu$  has been suppressed and the fluctuation of  $P_1$  has been written out explicitly to the correct order.

The simplest procedure for determining  $k$  has been covered previously (e. g. ref. 1) and will not be discussed here, except to note that it rests on comparison of the perturbed problem governed by eqs. (3.8) and (3.9) with the classical problem defined by

$$\frac{1}{S_c} \frac{d}{dz} \left( S_c \frac{d\hat{p}_\ell}{dz} \right) + k_\ell^2 \hat{p}_\ell = 0 \quad (3.12)$$

$$\frac{d\hat{p}_\ell}{dz} = 0 \quad (z = 0, L) \quad (3.13)$$

The calculation eventually produces the important formula for the complex wavenumber

$$k^2 = k_\ell^2 + \frac{1}{E_\ell^2} \left\{ \int_0^L \hat{p}_\ell \hat{h}_1 S_c dz + [S_c \hat{f}_1 \hat{p}_\ell]_0^L \right\} \quad (3.14)$$

where

$$E_\ell^2 = \int_0^L \hat{p}_\ell^2 S_c dz \quad (3.15)$$

From the real part of (3.14), one finds the results for the growth constant  $\alpha$ :

$$\begin{aligned} 2 \left( \frac{\alpha}{a} \right) \left( \frac{\omega}{a} \right) E_\ell^2 = & \left\{ -\bar{\rho} a k_\ell \left[ (\hat{u}^{(r)})_{p_\ell} + \frac{\bar{u} \hat{p}_\ell}{\rho a} \right] S_{be} \right\}_0^L \quad (1) \\ & + \bar{a} k_\ell \int_0^L \hat{p}_\ell \left[ \int \bar{m}_b(r) dq + \frac{R}{2} \Delta \hat{T}^{(r)} \int \bar{m}_b dq \right] dz \end{aligned}$$

$$\begin{aligned} & - \frac{k_\ell}{\rho a} \left\{ \int \hat{p}_\ell^2 + \frac{1}{2} \left( \frac{d\hat{p}_\ell}{dz} \right)^2 \right\} \int \bar{m}_b dq dz \quad (2) \star \\ & + \left\{ \int_0^L F^{(i)} \frac{d\hat{p}_\ell}{dz} S_c dz - \int_0^L U^{(i)} \frac{d\hat{p}_\ell}{dz} \int \bar{m}_b(p) dq dz \right\} \quad (3) \star \\ & + \frac{k_\ell}{a} \left\{ \frac{R}{c} \int_0^L \hat{p}_\ell \left[ \hat{e}_p^{(i)} \bar{w}_p + \bar{e}_p \hat{w}_p \right] + (\hat{Q}' + \hat{Q}_p^{(i)}) - \hat{p}_\ell \bar{w}_p \right\} S_c dz \\ & - \frac{\bar{a}}{k_\ell} \int_0^L (\hat{u} - \hat{u}_p^{(i)}) \bar{w}_p \frac{d\hat{p}_\ell}{dz} S_c dz \quad (4) \end{aligned} \quad (3.16)$$

Numerical results require values for the appropriate classical mode shape  $\hat{p}_\ell$  and wavenumber  $k_\ell^2$ . This involves preliminary calculations discussed further in § XI.

It is a familiar result for linear systems (see, e. g. refs. 1 and 11 for comments on the present application) that if  $\mathcal{E}$  represents the total acoustic energy in the chamber, then  $2\alpha$  is equal to the fractional rate of change of energy

$$2\alpha = \frac{1}{\mathcal{E}} \frac{d\mathcal{E}}{dt} \quad (3.17)$$

The numbered brackets in (3.16) have the following interpretations:

- (1) These are the coupling terms associated with surface combustion. The first terms are for end grains and the second are for lateral grains.
- (2) This represents a rate of change of acoustic energy, for the wave system in the chamber associated with the mass flux through the lateral boundary. For mass influx ( $\bar{m}_b$  positive) this represents a loss of energy, because the incoming flow must acquire energy. Conversely, this analysis formally shows that there is a gain of energy, if it is assumed that the exhaust flow has no acoustic energy after it crosses the boundary.
- (3) The first term represents the familiar dissipation of acoustic energy due to the force acting between particles and the gas. The second term is an energy loss due to the acquisition of acoustic energy by the particles flowing in at the boundary. It corresponds, for particulate matter, to the term 3 which is only for the gases.
- (4) These obviously represent the influences of residual combustion.

The preceding result has been used to examine the stability of small oscillations in motors as well as in T-burners. Some of the experiences will be discussed later in § IX. For the present, it is most important to note the presence of the starred terms which are peculiar to the one-dimensional problem. That is, they are associated with sources of mass at the boundary, flowing in or out normal to the direction of the motions within the chamber. The term in the first brackets represents the coupling between waves and combustion for a lateral element of surface.

By use of the perfect gas law and the defini-

tion of mass flux,  $m = \rho u$ , it is a simple matter to show that the coupling per unit area for end and lateral surfaces can be written (11)

end surface

(no parallel acoustic velocity)

$$-i\bar{\rho} \bar{a} k_{\ell} \left( \frac{\hat{m}_b}{\rho} + \gamma \frac{R}{\rho a} \Delta \hat{T} \bar{m}_b \right) \quad (3.18)$$

lateral surface

(acoustic velocity entirely parallel)

$$-i\bar{\rho} \bar{a} k_{\ell} \left( \frac{\hat{m}_b}{\rho} + \frac{R}{\rho a} \Delta \hat{T} \bar{m}_b \right) \quad (3.19)$$

These have been written in their complex forms, of which the real parts appear in eq. (3.16). It follows from (3.18) and (3.19) that if the processes are nonisentropic ( $\Delta T \neq 0$ ), then the formal representation of the coupling is different for the end and lateral surfaces: a factor  $\gamma$  multiplies  $\Delta T$  in (3.17). Hence, at least for this reason one must expect that the effective driving by surface combustion depends on the relative orientation of the surface element and the local acoustic field. This subject is pursued further in § IX.

The remaining starred terms in (3.16) arise, for flow entering the chamber, because the flow must turn from the direction normal to the surface into the axial direction. This involves a process of inelastic acceleration, which in the real situation occurs in some sort of boundary layer. A portion of the work done by the fluid in the chamber on that entering is dissipated. Hence, it may not be surprising that there is a net energy loss for the acoustic field, as shown. A more elaborate discussion of the meaning of the contributions to  $\alpha$  may be found in ref. 11.

In addition to the practical utility of the one-dimensional analysis, the features emphasized in the preceding paragraphs must be incorporated in the three-dimensional analysis. Contributions which are essentially due to processes occurring in boundary layers will arise in the latter case only if the complete equations are solved. That has not been done, and poses obviously complicated problems. Hence, the course followed here, based on ref. 11, is to patch the one-dimensional approximations onto the three-dimensional results. The vehicle for doing so is the formula for the complex wavenumber.

#### IV. Linear Three-dimensional Problems

The formulation based on linear classical acoustics in a nonuniform flow field has been most commonly used for stability analysis and, in one form or another, is the oldest<sup>(12-16)</sup>. Set  $\epsilon = 0$  in (2.13) and for harmonic motions, the equation to be solved is:

$$\nabla^2 \hat{p} + k^2 \hat{p} = \hat{h} \quad (4.1)$$

$$\hat{n} \cdot \nabla \hat{p} = -\hat{f} \quad (4.2)$$

where

$$\hat{h} = -\rho_0 \nabla \cdot (\vec{u} \cdot \nabla \vec{u} + \hat{u} \cdot \nabla \vec{u}) + i \frac{k}{a} \vec{u} \cdot \nabla \hat{p} + i \frac{\gamma k}{a_0} \hat{p} \nabla \cdot \vec{u} - i \frac{k}{a_0} \hat{p} \quad (4.3)$$

$$\hat{f} = i a_0 k \rho_0 \hat{u} \cdot \hat{n} + \rho_0 (\vec{u} \cdot \nabla \vec{u} + \hat{u} \cdot \nabla \vec{u}) \cdot \hat{n} - (\hat{F} - \hat{\sigma}) \cdot \hat{n} \quad (4.4)$$

As for the one-dimensional case, the formula for  $k^2$  is found by comparing this problem with the unperturbed classical problem governed by the equation and boundary condition

$$\nabla^2 \hat{p}_N + k_N^2 \hat{p}_N = 0 \quad (4.5)$$

$$\hat{n} \cdot \nabla \hat{p}_N = 0 \quad (4.6)$$

The formula for  $k^2$  is

$$k^2 = k_N^2 + \frac{1}{E_N} \left\{ \int \hat{p}_N \hat{h} dV + \oint \hat{p}_N \hat{f} dS \right\} \quad (4.7)$$

where

$$E_N = \int \hat{p}_N^2 dV \quad (4.8)$$

The imaginary part of (4.5) provides the result for the growth constant:

$$\begin{aligned} -2\alpha \frac{\omega}{a} E_N = & \star \\ & - \left\{ \bar{a} k_N \oint \hat{p}_N \left[ \hat{m}_b(r) + \frac{R \bar{m}_b}{a} \Delta \hat{T}(r) (\delta_{\parallel} + \gamma \delta_{\perp}) \right] dS \right\} \\ & + \left\{ \frac{k_N}{\rho a} \oint \left[ \hat{p}_N^2 + \frac{1}{k_N} (\nabla \hat{p}_N)^2 \right] \delta_{\parallel} \bar{m}_b dS - \frac{k_N}{a} \int \hat{p}_N^2 \nabla \cdot \vec{u} dV \right\} \\ & + \left\{ \oint \hat{u} \cdot \nabla \hat{p}_N \delta_{\parallel} \bar{m}_b dS - \int \hat{F} \cdot \nabla \hat{p}_N dV \right\} \\ & + \left\{ - \frac{k_N R}{a c_v} \int \hat{p}_N \left[ \hat{e}_p(r) \frac{\bar{w}_p}{\rho} + \hat{e}_p(r) \frac{\bar{w}_p}{\rho} + (\hat{Q}(r) + \hat{Q}(r)) \right] dV \right. \\ & \left. + \frac{k_N \gamma}{a} \int \hat{p}_N^2 \bar{w}_p dV + \int \bar{w}_p (\hat{u} \cdot \hat{u}) \cdot \nabla \hat{p}_N dV \right\} \quad (4.9) \end{aligned}$$

The starred terms in (4.9) in fact do not arise in the three-dimensional analysis indicated above, but have been carried over from the one-dimensional results, and correspond to the starred terms in (3.16). Difficulty in doing so arises because, as noted in § III, the lateral and end grains treated in the one-dimensional formulation are only special cases. To combine them in such a way as to accommodate an arbitrary relative orientation of the acoustic field and surface element, the weighting factors  $\delta_{\parallel}$  and  $\delta_{\perp}$  have been introduced. They are defined as

$$\delta_{\parallel} = \sin^2 \theta \quad (4.10)$$

$$\delta_{\perp} = \cos^2 \theta \quad (4.11)$$

where  $\theta$  is the angle between the local acoustic velocity and the normal direction to the surface. In terms of the local acoustic field, the angle  $\theta$  is computed from the formula (ref. 11, Appendix A)

$$\tan \theta = \left[ \frac{|\nabla_{\parallel} \cdot \hat{u}|}{|\nabla_{\perp} \cdot \hat{u}|} \right] \quad (4.12)$$

where  $\nabla_{\parallel}$  and  $\nabla_{\perp}$  are the gradient operators in the directions parallel and perpendicular to the surface, respectively.

For many practical configurations, the acoustic modes must be computed numerically (see

§ X ). The weighting factors  $\delta_{\parallel}$ ,  $\delta_{\perp}$  can be expressed in terms of the numerical results. Let  $n, s$  be the coordinates in the direction normal and parallel to the surface; the increments (mesh size) are  $\delta_n$ ,  $\delta_s$ . Then one can show that for the acoustic mode having frequency  $\omega$ ,

$$\begin{aligned}\nabla_{\parallel} \cdot \vec{u} &\approx \frac{1}{i\rho_o \omega} \frac{p(\delta n) - p(o)}{(\delta n)^2} \\ \nabla_{\perp} \cdot \vec{u} &\approx \frac{1}{i\rho_o \omega} \frac{p(s + \delta s) - p(s)}{(\delta s)^2}\end{aligned}\quad (4.13)$$

These give the values required at the position  $n = 0, s$ . The point is that  $\delta_{\parallel}$  and  $\delta_{\perp}$  can be computed for any acoustic mode. In special cases (such as for the modes in cylindrical ports), analytical formulas can be deduced.

The result for  $\alpha$  given as eq. (4.9) is the most general presently available for studying linear stability. It contains, by construction, the result (3.16) for one-dimensional problems. There are of course approximations involved, particularly in the manner in which the starred terms in (4.9) have been introduced. It has not yet been possible to evaluate their correctness. It appears, however, as discussed further in § X, that they may have significant influence on the numerical results.

It is to be noted that (4.9) exhibits explicitly contributions from all processes which are presently regarded as important. The terms representing residual combustion in a solid propellant motor (which is essentially all the combustion in a liquid propellant motor) are likely to be important in some cases, but little is known about the relevant processes.

#### V. Linear Analysis for High Mach Number of the Steady Flow

All of the work described to this point involves the assumption that the Mach number of the average flow is small. This of course does not mean that it has been neglected, nor does it mean that the steady flow has no influence on the acoustics. The complete results show the influence of the mean flow on both the complex wavenumber (frequency and growth rate) and on the mode structure. However, the great simplification achieved by considering only the first order effect of the mean flow is that the complex wavenumber for a particular mode can be calculated using only the unperturbed (classical) mode shape. This information can be obtained quite easily, either in closed form or by numerical computations.

The restriction to small Mach numbers is one which may be serious in many motors exhibiting combustion instability. It is not possible to give a precise meaning for "small," but probably the limit is around .2 - .3. This is well below values often attained, particularly early in firings of motors with low port-to-throat ratios. Extension of the analysis to higher Mach numbers is therefore a subject which must be considered, at least to gain an idea of how much additional work would be required. It happens, as shown here, that the necessary calculations, while requiring the use of a computer, are well within present capabilities. No numerical results are yet available. The purpose

here is to develop the necessary formalism and to demonstrate that more severe distortion of the acoustic field, by the mean flow, can be handled in a straightforward manner.

The procedure is again based on the general scheme outlined in § II. Only linear acoustics is considered, so the problem comes down to retaining higher order terms in the average Mach number. Here, only terms to order  $\mu^2$  are retained. This means that variations of the ambient mean flow properties with flow speed must be taken into account. As a first approximation, the steady field is assumed to be isentropic, so with  $( )_o$  denoting stagnation values, the average values are

$$\begin{aligned}\bar{T} &= T_o - T_o \left( \frac{\gamma - 1}{2} \right) \frac{\bar{u}^2}{a_o^2} \\ \bar{P} &= P_o - P_o \left( \frac{\gamma}{2} \right) \frac{\bar{u}^2}{a_o^2} \\ \bar{\rho} &= \rho_o - \rho_o \left( \frac{1}{2} \right) \frac{\bar{u}^2}{a_o^2} \\ \bar{a} &= a_o^2 - \left( \frac{\gamma - 1}{4} \right) \bar{u}^2\end{aligned}\quad (5.1)$$

The expansions used in the complete conservation equations are therefore (5.1) plus the perturbations; for example, with the ordering parameters  $\mu$  and  $\epsilon$  shown,

$$p = p_o - \mu^2 \left( \frac{\gamma P_o}{2} \right) \frac{\bar{u}^2}{a_o^2} + \epsilon p', \text{ etc.} \quad (5.2)$$

The perturbation,  $p'$ , must also be expanded to second order in  $\mu$ . However, it will be seen shortly that only the terms to first order in  $\mu$  are required to compute the wavenumber to second order.\*

Substitution of the expansions in the wave equation (2.13) leads eventually ( $\epsilon \rightarrow 0$ ) to

$$\begin{aligned}\nabla^2 p' - \frac{1}{a_o^2} \frac{\partial^2 p'}{\partial t^2} &= \mu \left\{ \frac{\bar{u}}{a_o} \cdot \nabla \left( \frac{\partial p'}{\partial t} \right) + \frac{\gamma}{2} \frac{\partial p'}{\partial t} \nabla \cdot \vec{u} \right. \\ &\quad \left. - \rho_o \nabla \cdot (\vec{u} \cdot \nabla \vec{u}' + \vec{u}' \cdot \nabla \vec{u}) - \frac{1}{2} S_1 \right\} \\ &\quad - \mu^2 \left\{ \frac{\gamma}{2} p' \nabla \cdot (\vec{u} \cdot \nabla \vec{u}) - \frac{\gamma - 1}{2 a_o^2} \bar{u}^2 \nabla^2 p' \right. \\ &\quad \left. + \nabla p' \cdot \nabla \frac{\bar{u}^2}{2} + \frac{1}{2} \frac{\rho_o}{T_o} T' \nabla^2 \bar{u}^2 + \frac{1}{2} S_2 \right\}\end{aligned}\quad (5.3)$$

where  $S_1$  and  $S_2$  are the first and second order terms in the expansion of  $S$ .

\* This is a general feature of the techniques used here. The eigenvalue ( $k^2$ ) can be calculated to one order higher than the eigenfunction ( $p'$ ).

$$S = \frac{\partial P}{\partial t} - \gamma p \nabla \cdot \left( \frac{\vec{F} - \vec{\sigma}}{\rho} \right) = \bar{S} + \epsilon [\mu S_1 + \mu^2 S_2] \quad (5.4)$$

There are no terms in  $S$  independent of the mean flow speed. The explicit forms of  $S_1$  and  $S_2$  can easily be worked out, but they will not be shown here.

Expansion of the momentum equation (2.5) to the same order leads to

$$\frac{\partial \vec{u}'}{\partial t} + \frac{1}{\rho_0} \nabla p' = -\mu \left\{ \vec{u}' \cdot \nabla \vec{u}' + \vec{u}' \cdot \nabla \vec{u} - (\vec{F}'_1 - \vec{\sigma}'_1) \right\} + \mu^2 \left\{ \frac{1}{2} \frac{\rho}{\rho_0} \nabla u'^2 + \frac{u'^2}{2\rho_0} \nabla p' + (\vec{F}'_2 - \vec{\sigma}'_2) \right\} \quad (5.5)$$

for which the perturbation of  $(\vec{F} - \vec{\sigma})/\rho$  has been written

$$\left[ \frac{1}{\rho} (\vec{F} - \vec{\sigma}) \right]' = \epsilon \mu (\vec{F}'_1 - \vec{\sigma}'_1) + \epsilon \mu^2 (\vec{F}'_2 - \vec{\sigma}'_2) \quad (5.6)$$

Equation (5.5) is used in two ways: first to fix the boundary condition on  $p'$ , and second to compute the mode shape  $\vec{u}'$  including corrections for higher Mach number. The boundary condition is set by taking the component of (5.5) normal to the surface, thus producing a formula for  $\hat{n} \cdot \nabla p'$ .

For harmonic motions, (5.3) may be written in the form

$$\nabla^2 \hat{p} + k^2 \hat{p} = \mu \hat{h}_{\mu 1} + \mu^2 \hat{h}_{\mu 2} \equiv \hat{h} \quad (5.7)$$

and the boundary condition from (5.3) is

$$\hat{n} \cdot \nabla \hat{p} = -\mu \hat{f}_{\mu 1} - \mu^2 \hat{f}_{\mu 2} \equiv -\hat{f} \quad (5.8)$$

The most convenient method of solution is a perturbation iteration approach based on using a Green's function expanded in the unperturbed acoustic model (ref. 17, chapter 9, and ref. 16). The Green's function  $G(\vec{r}/\vec{r}_0)$  satisfies the equation and boundary condition:

$$\nabla^2 G + k^2 G = \delta(\vec{r} - \vec{r}_0), \quad (5.9)$$

$$\hat{n} \cdot \nabla G = 0 \quad (5.10)$$

By standard operations, the formal solution to (5.7) can be written

$$\hat{p} = \int \hat{h} G dV + \oint \hat{f} G dS \quad (5.11)$$

The expansion for  $G$  in terms of the  $\hat{p}_N$  (determined from (4.3) and (4.4)) is

$$G(\vec{r}/\vec{r}_0) = \sum_N \frac{\hat{p}_N(\vec{r}) \cdot \hat{p}_N(\vec{r}_0)}{E_N^2(k^2 - k_N^2)} \quad (5.12)$$

Suppose one is interested in the  $n^{\text{th}}$  mode, so that  $\hat{p}$  is nearly equal to  $\hat{p}_N$ . Substitute (5.12) into (5.11) and split off the  $n^{\text{th}}$  mode from the series:

$$\hat{p} = \hat{p}_N \left[ \frac{1}{E_n^2(k^2 - k_n^2)} \left\{ \int \hat{p}_n \hat{h} dV + \oint \hat{p}_n \hat{f} dS \right\} + \sum_{N \neq n} \frac{\hat{p}_N}{E_N^2(k^2 - k_N^2)} \left\{ \int \hat{p}_N \hat{h} dV + \oint \hat{p}_N \hat{f} dS \right\} \right] \quad (5.13)$$

But  $\hat{p}(\vec{r})$  should have the form  $\hat{p} \sim \hat{p}_N$  plus corrections, a requirement which produces both a formula for  $k^2$  and an expression for  $\hat{p}$ :

$$k^2 = k_n^2 + \frac{1}{E_n^2} \left\{ \int \hat{p}_n \hat{h} dV + \oint \hat{p}_n \hat{f} dS \right\} \quad (5.14)$$

$$\hat{p}(\vec{r}) = \hat{p}_n(\vec{r}) + \sum_{N \neq n} \frac{\hat{p}_N(\vec{r})}{E_N^2(k^2 - k_N^2)} \left\{ \int \hat{p}_N \hat{h} dV + \oint \hat{p}_N \hat{f} dS \right\} \quad (5.15)$$

These results are the basis for the iterative solution, for  $\hat{h}$  and  $\hat{f}$  have been expanded in powers of  $\mu$  according to (5.7) and (5.8). Hence, (5.14) is

$$k^2 = k_n^2 + \frac{\mu}{E_n^2} H_n^{(1)} + \frac{\mu^2}{E_n^2} H_n^{(2)} \quad (5.16)$$

Similarly, the mode shape is

$$\hat{p} = \hat{p}_n + \mu \sum_{N \neq n} \frac{\hat{p}_N}{E_N^2(k^2 - k_N^2)} H_N^{(1)} + \mu^2 \sum_{N \neq n} \frac{\hat{p}_N}{E_N^2(k^2 - k_N^2)} H_N^{(2)} \quad (5.17)$$

where

$$H_N^{(1)} = \int \hat{p}_N \hat{h}_{\mu 1} dV + \oint \hat{p}_N \hat{f}_{\mu 1} dV \quad (5.18)$$

$$H_N^{(2)} = \int \hat{p}_N \hat{h}_{\mu 2} dV + \oint \hat{p}_N \hat{f}_{\mu 2} dV$$

The wavenumber  $k$  can be eliminated from (5.17) by using (5.16), and the mode shape (5.17) can be written to second order in  $\mu$  as

$$\hat{p}(\vec{r}) = \hat{p}_n(\vec{r}) + \mu \sum_{N \neq n} \frac{\hat{p}_N}{E_N^2(k_n^2 - k_N^2)} H_N^{(1)} + \mu^2 \sum_{N \neq n} \frac{\hat{p}_N}{E_N^2(k_n^2 - k_N^2)} \left[ H_N^{(2)} - \frac{H_n^{(1)} H_N^{(1)}}{E_n^2(k_n^2 - k_N^2)} \right] \quad (5.19)$$

Numerical results for stability of waves are of course found from the real part of (5.16); but to evaluate  $H_n^{(1)}$  and  $H_n^{(2)}$ , the mode shapes  $\hat{p}$  and  $\vec{u}$  must be known for substitution in  $\hat{h}$  and  $\hat{f}$  under the integrals appearing in (5.18). Now since  $H_n^{(1)}$  is already multiplied by  $\mu$ , only the mode shape with first order corrections is required in  $H_n^{(1)}$ ; and since  $H_n^{(2)}$  is multiplied by  $\mu^2$ , the unperturbed mode shape ( $\hat{p}_n$ ) is used in that term.

The mode shape including the first order correction is given by (5.19) with the terms in  $\mu^2$  dropped, and the unperturbed mode shapes used to evaluate the  $H_n^{(1)}$ . Hence, all that is required of the acoustics calculations is the set of unperturbed acoustic modes. To calculate the wavenumber to first order in the Mach number, only the single unperturbed mode is required; but the second order calculation uses all of the unperturbed modes in order to compute the perturbed mode shape to first order. In fact, of course, only a finite number of modes can be used in practice. How many are necessary for, say, five per cent accuracy cannot easily be answered without carrying out the calculation. Note that the contributions from the higher harmonics in the first sum of (5.17) decrease because the wavenumber increases.

For example, for longitudinal modes,  $k_N = N\pi/L$ , where  $L$  is the length of the chamber; so if one is studying the fundamental mode ( $n = 1$ ),

$$\frac{1}{k_n^2 - k_N^2} = \frac{1}{(\pi/L)^2} \frac{1}{1 - N^2}$$

The first ten modes would likely be sufficient. This requirement is easily and cheaply met with current numerical techniques. It is possible that more modes are required for more complicated configurations, because they often tend to be more closely spaced in frequency.

## VI. Numerical Calculations of Nonlinear Combustion Instability

The large source of energy in a solid-propellant rocket motor, and the relatively weak dissipative mechanisms, imply that unstable motions must be anticipated. Indeed, it is probably a fair statement that the majority of motor designs have, at one time or other, exhibited instabilities. Under these circumstances, it becomes important to learn how to control, reduce, or suppress the oscillations. Thorough understanding necessarily involves studying the nonlinear processes.

There are several very interesting features of the observed waveforms which should be noted. Linear behavior, in the sense that the amplitude of unstable waves grows proportionately to  $\exp(\alpha t)$ , commonly persists to much higher amplitudes than one would expect. This has been seen in motors of all sizes, as well as in T-burners. Second, even at quite large amplitudes (up to 20% and more of the mean pressure) the waves often have remarkably little distortion and harmonic content. The transient periods of growth to limiting amplitudes are in many cases (see § X) accurately approximated by the behavior of a nonlinear oscillator. There are other peculiarities, such as relatively slow changes of the limiting amplitude, non-exponential variations of the amplitude subsequent to pulsing, and DC shifts of the pressure which must also be related ultimately to nonlinear processes.

That much of the obvious nonlinear behavior is delayed to the rather high amplitudes noted above is contrary to what one would expect on the basis of classical acoustics in the absence of combustion and mean flow. For example, in a simple resonance tube driven by a piston at one end, distortion of the waveform may be clearly observed at amplitudes as low as 6 - 8% of the average pressure. This reflects the generation of harmonics caused by the gasdynamic nonlinearities; these are mainly associated with the convective motions (e. g.  $u \cdot \nabla u$ ) and variations of the speed of sound. Hence, the coupling between the waves, combustion, and mean flow, must act not only to produce growth of some waves, but simultaneously either to attenuate or at least retard the growth of waves at higher frequencies. On the basis of the known qualitative characteristics of the dynamics of surface combustion (§ VIII), this is an appealing supposition.

The correct interpretation of the behavior can not be established without the aid of analysis. In the next section, a method for approximately computing nonlinear behavior is outlined. However, owing to the assumptions required to simplify the work (some of which have already been covered),

confidence in the results is not complete without an "exact" solution serving as a check. It is the purpose of this section to summarize some recent work on a numerical analysis of nonlinear behavior (ref. 18).

Owing to the complicated nature of the calculations, only the one-dimensional problem has been treated. The complete nonlinear equations for one-dimensional flow, which have been treated in ref. 18, are the following:

$$\text{conservation of mass (gas)} \quad \frac{\partial}{\partial t}(\rho S_c) + \frac{\partial}{\partial z}(\rho u S_c) = w + w_p S_c \quad (6.1)$$

$$\text{conservation of mass (particles)} \quad \frac{\partial}{\partial t}(\rho_p S_c) + \frac{\partial}{\partial z}(\rho_p u_p S_c) = w^{(p)} - w_p S_c \quad (6.2)$$

$$\text{conservation of momentum} \quad \rho \frac{\partial u}{\partial t} + \rho u \frac{\partial u}{\partial z} + \frac{\partial p}{\partial z} = F - \sigma_1 \quad (6.3)$$

$$\begin{aligned} \text{conservation of energy} \quad & \rho c_v \frac{\partial T}{\partial t} + \rho u c_v \frac{\partial T}{\partial z} + \frac{p}{S_c} \frac{\partial}{\partial z}(u S_c) \\ & = \left( \frac{a_0^2}{\gamma} + \Delta e_0 \right) \frac{w}{S_c} + (e_{p0} - e_{o0}) w_p + (Q + Q_p) \end{aligned} \quad (6.4)$$

Equations (6.1) - (6.4) were solved, in the case of unsteady motion, by using the method of characteristics. The following additional assumptions were used.

- (i) No residual combustion:  $w = Q = 0$ . The energy exchange  $Q_p$  then represents heat transferred between the particulate matter and the chamber gases.
- (ii) Uniform port:  $S_c = \text{constant}$ .
- (iii) The speeds of the gas and particles vanish at  $z = 0$ .
- (iv) The nozzle flow is computed using the constant fractional lag approximation for the two-phase flow.
- (v) The nozzle behaves in a quasi-steady manner.
- (vi) The transient burning response is given by the simplest result quoted below (eq. (8.1)). Hence, the combustion response is assumed to be linear. Although most results are for pressure coupling, there are some preliminary calculations using a very simple model for velocity coupling (see § VIII).
- (vii) Only a single particle size is treated. Both linear and nonlinear drag laws have been examined.

The program developed in ref. 19 computes first the steady-state flow field, and then the unsteady behavior subsequent to initial disturbances. Both standing waves and pulses have been analyzed. Although some of the results have been obtained with a view to interpreting a series of tests with small-scale motors<sup>(19)</sup>, much of the work has been devoted to special cases. These have served to verify the correctness of the program and have emphasized the relative importance of the various contributions.

In particular, it appears crucial to take proper account of the transient burning characteristics.

The form used, eq. (8.1), typically has a peak, of which the width, height, and location in frequency depend strongly on the two parameters A and B. The tendency of the burning propellant to drive waves falls off rapidly with increasing frequency, and indeed, the combustion process may attenuate the waves. It seems at the present time that this is the reason for the low harmonic content remarked upon above. The numerical results obtained to date support this conclusion, but more detailed work remains to be done.

Since the instantaneous burning rate depends on the past history, much information must be stored during a calculation, and the computing time required for this is significant. Hence, the transient response was handled in this work in a manner which would be unsuitable for analytical work. The frequency response, eq. (8.1), can be treated as a Laplace transform, with the variable  $s = i\Omega$ . The inverse transform then gives an explicit formula for the fluctuation of mass flux in response to an arbitrary pressure fluctuation:

$$\frac{1}{nAB} \frac{m'}{\bar{m}}(\tilde{t}) = \frac{1}{2\pi i} \int \frac{\lambda(s)}{[\lambda^2 + (AB - A - 1)\lambda + A]} \frac{p'}{\bar{p}}(s) e^{s\tilde{t}} d\tilde{t} \quad (6.5)$$

The difficulty in using this formula is that the kernel introduces complex error functions which, for the sort of calculations required in this work, are uneconomical to handle numerically.

This problem has been overcome in ref. 19 by rewriting the Laplace transform in such a way that inversion leads to an implicit formula for the perturbation of mass flux:

$$\begin{aligned} \frac{m'}{\bar{m}}(\tau) = & \frac{\sigma_1 + \sigma_2}{\sqrt{\pi}} \int_0^\tau \frac{m'}{\bar{m}}(\tau - \xi) \frac{e^{-\xi}}{\sqrt{\xi}} d\xi - \sigma_1 \sigma_2 e^{-\tau} \int_0^\tau \frac{m'}{\bar{m}}(\xi) e^{\xi} d\xi \\ & + 2nAB \left\{ \frac{1}{\sqrt{\pi}} \int_0^\tau \frac{p'}{\bar{p}}(\tau - \xi) \frac{e^{-\xi}}{\sqrt{\xi}} d\xi + e^{-\tau} \int_0^\tau \frac{p'}{\bar{p}}(\xi) e^{\xi} d\xi \right\} \end{aligned} \quad (6.6)$$

This is an exact result, showing obviously the dependence on the history of burning. The accuracy of the numerical calculations has been checked against special cases which can be expressed in closed form.

Equation (6.6) is therefore the linear boundary condition used in the numerical analysis for pressure coupling. The transient behavior of the burning is due solely to the thermal wave in the solid phase (see § VIII). For the calculations with velocity coupling, it was assumed that the thermal wave again dominated, and the only change is that  $p'/\bar{p}$  is replaced by a suitable function of the velocity field:

$$p'/\bar{p} \rightarrow \epsilon_1 (|u| - u_t) - \epsilon_2 (|\bar{u}| - u_t) \quad (6.7)$$

where  $u_t$  is the threshold velocity and

$$\begin{aligned} \epsilon_1 = & \begin{cases} 0 & |u| < u_t \\ 1 & |u| > u_t \end{cases} \\ \epsilon_2 = & \begin{cases} 0 & |\bar{u}| < u_t \\ 1 & |\bar{u}| > u_t \end{cases} \end{aligned} \quad (6.8)$$

This formulation then accounts for rectification<sup>20-23</sup>, but none of the important physical processes associated with the parallel flow. Better representations will be incorporated later in the work which is continuing.

Some examples of the results which have been obtained so far are shown in Figs. 1-3. Figure 1 shows a pressure trace for an unstable mode, the initial condition having the form of a standing wave at the fundamental frequency of the chamber. For the conditions chosen, the second mode is stable, as shown by Fig. 2. The initial disturbance contained equal parts of first and second modes, but

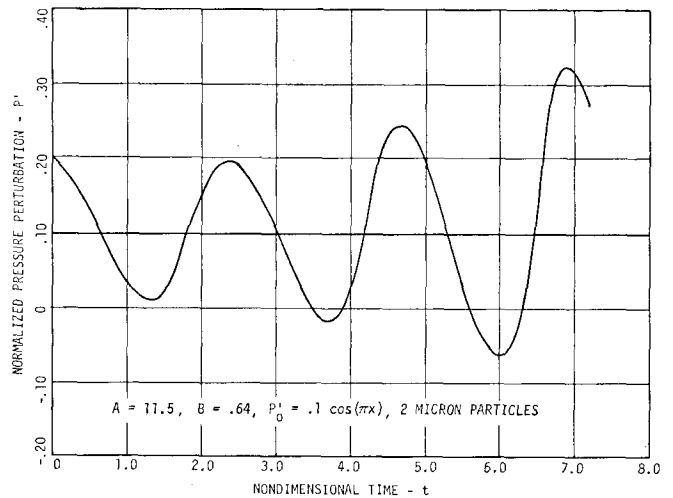


Fig. 1 Numerical Result for an Unstable Fundamental Mode (ref. 18).

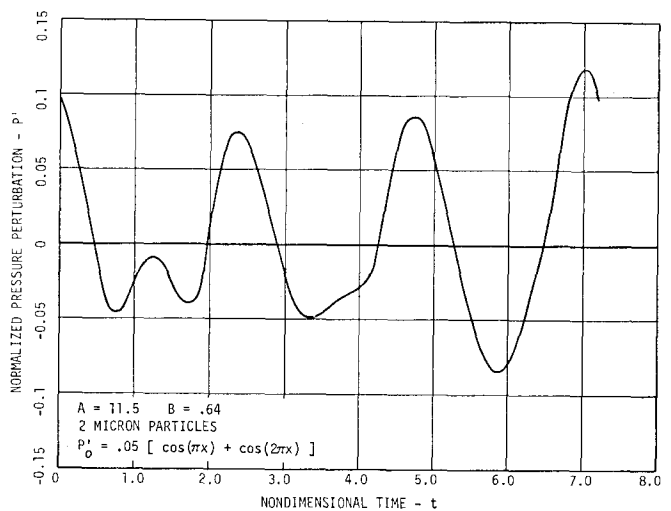


Fig. 2 Numerical Result for an Unstable Fundamental Mode and Stable Second Harmonic (ref. 18).

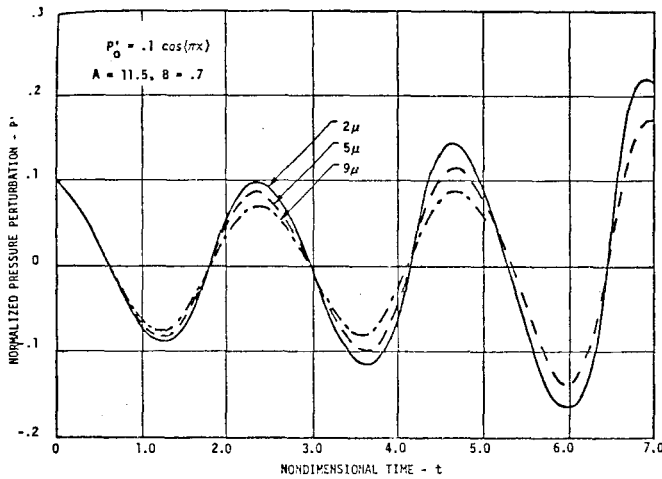


Fig. 3 Influence of Particle Size on the Growth of an Unstable Mode (ref. 18).

after three cycles, the pressure contains almost no second harmonic. The transient combustion coupling is apparently crucial to this behavior; the response function for the values of A and B shown is quite large at the fundamental frequency and small at the frequency of the second mode. It may be noted also that the amplitude of the pressure does not immediately begin to grow; there is even a slight decrease after one cycle. The reason for this is that it takes several cycles for the transient burning rate to attain the value approximating that due to the pressure disturbance introduced. Only after a time somewhat longer than one cycle is the response sufficient to cause the wave to grow.

Figure 3 shows the important effect of changing particle size. The traces shown were calculated for the complete problem of an unstable disturbance in a motor. The increased attenuation for increasing particle size is qualitatively consistent with the predictions of work on particle damping (refs. 24-26).

### VII. Approximate Analysis of Nonlinear Combustion Instability

The calculations discussed in this section are in progress<sup>(27)</sup>; although the formalism is complete, no numerical results are yet available. Mainly, the purpose here is to convey the gist of the analysis and to demonstrate that the approach taken has considerable promise.

Only a bare outline of the procedure is covered here. The formulation is given for the three-dimensional case, but the special contributions arising in the one-dimensional problem (see § III) are included. Hence, an approximate nonlinear analysis for one-dimensional problems can be extracted for comparison with the numerical analysis discussed in the preceding section. This is, in fact, potentially an important use for the numerical analysis, namely, to check the validity of the approximate calculations. If satisfactory agreement can be established, then the approximate calculations can be used to study three-dimensional

problems which cannot be handled economically by numerical techniques.

Since this analysis has been done, it has become evident that the techniques used are essentially those referred to generically as the methods of weighted residuals, of which the best known is the Galerkin method. Use of the Galerkin method for studying nonlinear instabilities in liquid propellant rockets has been reported in refs. 28-30. There are, however, several important differences in the present work.

First, the basis for all the calculations is the single nonlinear wave equation (2.10) for the pressure field. The expansion of (2.10) to first order in  $\mu$  and second order in  $\epsilon$  leads to eq. (2.13). Because terms of higher order in  $\mu$  and  $\mu\epsilon$ ,  $\mu\epsilon^2$ , etc. have been dropped, it is sufficient for calculating the amplitude and frequency of  $p'$  to use functions for both  $p'$  and  $\vec{u}'$  in which the spatial structure is independent of the mean flow speed. This is essentially the same conclusion discussed in § IV. In ref. 31 this argument was used as the basis for a calculation using a single mode approximation; but in general, many modes are present, and the more general form of solution is

$$\frac{p'}{p_0} = \sum_{i=0}^{\infty} \eta_i(t) \hat{p}_i(\vec{r}) \quad (7.1)$$

$$\vec{u}' = \sum_{i=0}^{\infty} \frac{\dot{\eta}_i(t)}{\gamma k_i} \nabla \hat{p}_i(\vec{r}) \quad (7.2)$$

where the  $\hat{p}_i(\vec{r})$  are the unperturbed classical modes. Note that (7.1) and (7.2) satisfy the classical acoustic equations. The problem here is to find the time dependence  $\eta_i(t)$  of each of the modes. Naturally, the actual pressure and velocity mode shapes have, in addition to (7.1) and (7.2), corrections proportional to  $\mu$ . These approximations are also valid if higher order terms in  $\epsilon$  are retained in the nonlinear wave equation, providing that only terms linear in  $\mu$  are retained and those of order  $\mu\epsilon$ ,  $\mu\epsilon^2$ , etc. are dropped.

The next step after substitution of these approximations is to multiply eq. (2.13) by  $\hat{p}_n$  and integrate over the volume of the chamber. This eventually produces the nonlinear equation for  $\eta_n$ :

$$\begin{aligned} \ddot{\eta}_n + \omega_n^2 \eta_n - \frac{1}{E_n^2} \left\{ \sum_{i=0}^{\infty} D_{ni} \dot{\eta}_i + \oint_{\hat{p}_N} \frac{\partial}{\partial t} [a_0^2 m_b' + R\Delta T' \bar{m}_b (\delta_{\parallel} + \gamma \delta_{\perp})] dS \right. \\ \left. + a_0^2 \int \vec{u}' \cdot \nabla \hat{p}_n \bar{w}^{(p)} \delta_{\parallel} dS \right\} \\ - \frac{1}{\gamma E_n^2} \sum_{i=0}^{\infty} \sum_{j=0}^{\infty} \left[ \frac{1}{k_i h_j} I_{nij} \dot{\eta}_i \dot{\eta}_j - a_0^2 J_{nij} \eta_i \eta_j \right] \\ - \left[ \int \hat{p}_n h_v dV + a_0^2 \oint_{\hat{p}_N} \hat{p}_n f dS \right] = 0 \quad (7.3) \end{aligned}$$

where

$$D_{ni} = \int \left[ \frac{k_n^2}{2} \hat{p}_n \vec{u}_n - \nabla \hat{p}_i \cdot \hat{p}_i \vec{u}_i - \nabla \hat{p}_n \right] dV - \int \hat{p}_n \hat{p}_i \nabla \cdot \vec{u} dV$$

$$+ \gamma \int \hat{p}_n \hat{p}_i \frac{\bar{w}}{\rho_0} dV + \frac{1}{\rho_0} \oint \left[ \hat{p}_n \hat{p}_i + \frac{1}{k_i^2} (\nabla \hat{p}_i) \cdot (\nabla \hat{p}_n) \right] \bar{m}_b \delta_{ij} dS$$
(7.4)

$$I_{nij} = \frac{1}{2} (k_n^2 + k_i^2 + k_j^2) \int \hat{p}_n (\nabla \hat{p}_i) \cdot (\nabla \hat{p}_j) dV - \gamma k_i^2 k_j^2 \int \hat{p}_n \hat{p}_i \hat{p}_j dV$$
(7.5)

$$J_{nij} = \frac{1}{2} (k_n^2 - \gamma (k_i^2 + k_j^2)) \int \hat{p}_n \hat{p}_i \hat{p}_j dV - \int \hat{p}_n (\nabla \hat{p}_i) \cdot (\nabla \hat{p}_j) dV$$
(7.6)

$$h_v = -\frac{1}{\epsilon} \left[ \frac{\partial P'}{\partial t} - a_0^2 \nabla \cdot (\vec{F}' - \vec{\sigma}') \right]$$
(7.7)

$$f_v = -\frac{1}{\epsilon} (\vec{F}' - \vec{\sigma}') \cdot \hat{n}$$
(7.8)

The additional contributions from the one-dimensional problem have been incorporated in (7.3) according to the argument of § IV. For simplicity, the functions  $h_v$  and  $f_v$ , containing the influences of residual combustion and gas/particle interactions, have not been expanded; and in (7.3) the parameters  $\mu$  and  $\epsilon$  have again been suppressed.

Unlike the work on liquid rockets cited above, a single equation corresponding to (7.3) can be used for calculations to higher order in  $\epsilon$ . Those works made use of the original differential equations rather than the nonlinear wave equation, and hence in higher order approximations became considerably more complicated at this point. And of course, another important difference is that the formulation here accounts for the influences of particulate matter, surface combustion, and the nonuniform flow field necessarily present in a solid propellant rocket motor.

The method used to obtain the time-dependent amplitudes also differs from that used in the references cited and, particularly for approximations to higher order in  $\epsilon$ , is considerably simpler. Results for comparable problems should be essentially the same, although this point has not been checked. The discussion here is less involved, and the method is illustrated sufficiently well, by considering the special case in which only a single mode is included in the expansions (7.1) and (7.2). Also, the term containing  $h_v$ ,  $f_v$ , and  $\bar{w}^{(p)}$ , will be dropped. All subscripts can be suppressed since only the values  $i=j=n$  are allowed; hence, eq. (7.3) becomes

$$\ddot{\eta} + \omega^2 \eta - \frac{1}{E} \left\{ D \dot{\eta} + \oint \hat{p} \frac{\partial}{\partial t} [a_0^2 m_b^2 + R \Delta T' \bar{m}_b (\delta_{||} + \gamma \delta_{\perp})] dS \right.$$

$$\left. - \frac{1}{\gamma E^2} \left[ \frac{1}{k^4} I \eta^2 - a_0^2 J \eta^2 \right] \right\} = 0 \quad (7.9)$$

The most useful methods of solution rely on the observation that for small perturbations of the sort characterized by the linear terms in  $\mu$  and the nonlinear terms in  $\epsilon$ , the solution to (7.9) is basically harmonic, being dominated by the combination  $\ddot{\eta} + \omega^2 \eta$ . The remaining terms cause relatively slow changes in the amplitude; "relatively slow" means that the fractional change of amplitude is small in one cycle of the oscillation. These terms

can be regarded as the force  $F$  acting on the harmonic oscillator having natural frequency  $\omega$ . The equation for  $\eta$  is

$$\ddot{\eta} + \omega^2 \eta = \vec{F} \quad (7.10)$$

and the solution is assumed to have the form

$$\eta \approx A(t) \sin(\omega t + \phi(t)) \quad (7.11)$$

By either a method of averaging (e. g. ref. 32) or by the technique of expanding in two time variables<sup>(33)</sup>, differential equations for  $A$  and  $\phi$  can be deduced. It is really the amplitude which is most useful here, and by the first method one finds the first approximation for the equation satisfied by  $A(t)$ :

$$\frac{dA}{dt} = \frac{1}{2\pi\omega} \int_0^{2\pi} F(A \sin \psi, \omega A \cos \psi) \cos \psi d\psi \quad (7.12)$$

where  $\psi = \omega t + \phi$ .

This equation is essentially an approximate statement of the conservation of energy for the harmonic oscillator governed by (7.10). To see this, assume that the amplitude, frequency, and phase change little during a cycle. Then the time-averaged total energy is  $\omega^2 A^2/2$  and it changes at the rate  $\omega A \dot{A}$ . The rate of doing work is force times velocity,  $F \dot{\eta} \approx F \omega A \cos(\omega t + \phi) = F \omega A \cos \psi$ ; but the average (over one period  $\tau = 2\pi/\omega$ ) of  $F \dot{\eta}$  is

$$\frac{1}{T} \int_t^{t+T} F \omega A \cos(\omega t + \phi) dt = \frac{\omega A}{2\pi} \int_0^{2\pi} F \cos \psi d\psi$$

which must equal the rate of change of time-averaged energy. This condition produces eq. (7.12).

For problems in which two or more modes are accounted for, there is an "oscillator" corresponding to each mode, whose behavior is governed by eq. (7.3). The approximate time dependence of the amplitudes of these oscillators can be found by application of eq. (7.12) to each oscillator. It is on this basis that the following remarks are made.

First, it can be shown that the linear terms in eqs. (7.9) and (7.3) reproduce exactly the formula for the growth constant given by eq. (4.7). To do so requires that the combustion coupling terms ( $m_b^2$  and  $\Delta T'$ ) be replaced by functions proportional to  $p'$  and hence  $\eta$ . That is, the response of the combustion processes is assumed to be that of a harmonic disturbance which has been applied for a very long time in the past. Thus, the history of the motions, in the sense discussed in § VII, is ignored, just as it is in the linear stability analysis. The more accurate transient behavior can be accounted for at the expense of increased computational labor.

When the nonlinear terms of (7.9) are included, eq. (7.12) gives an equation for  $A$  having the form

$$\frac{dA}{dt} = \alpha A - \beta A^2 = \beta A \left( \frac{\alpha}{\beta} - A \right) \quad (7.13)$$

For  $\beta=0$ ,  $A \sim \exp(\alpha t)$  in accord with the assertion of the preceding paragraph. For non-zero  $\beta$ , the qualitative behavior can be seen easily from the phase plot, a graph of  $dA/dt$  given by (7.13) vs.  $A$ . Figure 4 shows the two possible cases of interest for  $\beta/\alpha > 0$ . If  $\alpha > 0$ , a small disturbance is unstable and develops into a limit cycle, a steady oscillation having amplitude  $\alpha/\beta$ . The arrows show the motion

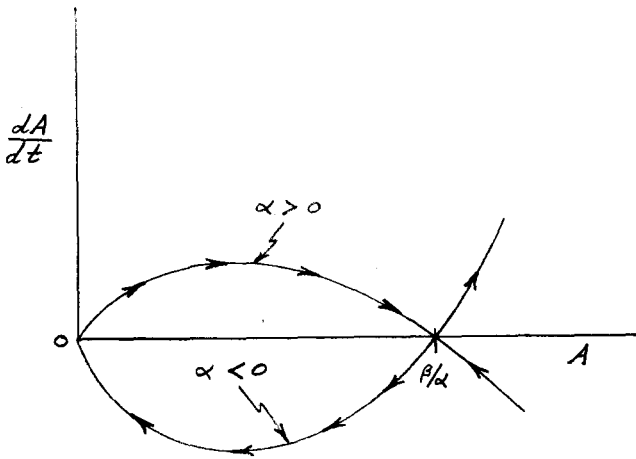


Fig. 4 Phase Plot for Equation (7.13).

of the system. In this approximation, then, the limiting amplitude is proportional to the linear growth constant. There is some experimental evidence supporting this conclusion, but it is not generally valid.

If the acoustic expansion is carried out to third order, producing terms in  $\eta^3, \eta^3, \eta\eta^2$ , etc., the equation for the amplitude has the form

$$\frac{dA}{dt} = \alpha A - \beta A^2 + \gamma A^3 = A(A - A_1)(A - A_2) \quad (7.14)$$

where the constants  $A_1, A_2$  depend on the flow field and possible nonlinear "forces" such as viscous effects at inert surfaces. The phase plot, shown in Figure 5 for  $A_1, A_2 > 0$ , now has a qualitatively new feature. For  $\alpha < 0$ , small disturbances are stable. But the system is linearly unstable, since if the initial amplitude is greater than  $A_1$ , the ultimate motion is a limit cycle with amplitude  $A_2$ . This "triggering" feature has been discussed in the work on liquid rockets. The conclusion here is consistent with those numerical results: in the single mode approximation, triggering limits are found only if the acoustics is carried out to third order.

That a finite amplitude disturbance may be required to produce an unstable motion has been observed. Quite extensive measurements have been reported in ref. 9 and earlier works, but there is presently no theoretical interpretation available.

Now, in fact, harmonics are probably always generated. A limited amount of harmonic analysis of T-burner test records has shown that in many cases, when no distortion is obvious in oscillograph records, there may in fact be higher harmonics present having amplitudes as large as 5 to 10%. A contribution to the nonlinear coupling of harmonics is contained in (7.3). For example, if two modes are accounted for, the equations for the

amplitudes have the form

$$\begin{aligned} \frac{dA_1}{dt} &= \alpha_1 A_1 - \beta_1 A_1^2 + C_{12} A_1 A_2 \\ \frac{dA_2}{dt} &= \alpha_2 A_2 - \beta_2 A_2^2 + C_{21} A_1 A_2 \end{aligned} \quad (7.15)$$

The coupling terms arise from processes causing a transfer of energy between modes. Once again, spontaneous growth to a limit cycle is possible, although the behavior is more complicated and varies considerably with the values of the constants. The phenomenon of triggering is not contained in this simple picture; it is necessary to go to the third-order approximation, no matter how many modes are included.

It seems likely, however, that if a more accurate representation of the transient combustion dynamics is used, "triggering" or nonlinear instability (when the system is linearly stable) may be found. Some support for this speculation may be found in refs. 28-30, which did incorporate a time lag in the combustion coupling. However, in those works, a constant time lag was used, and it is well known that surface combustion responds with a time lag depending on frequency. (That is essentially the reason for the complications discussed in connection with eqs. (6.5) and (6.6).)

The single-mode approximation, expressed essentially by eq. (7.14), has already been usefully applied to T-burner tests. It does appear, however, that harmonic coupling must be accounted for to obtain wholly satisfactory results (see § X).

Only the nonlinearities associated with the gas-dynamics have been explicitly shown here. It is known from measurements<sup>(34)</sup> that nonlinear surface heat transfer is significant in T-burners. Quite possibly, nonlinear behavior of the particulate matter may be important in motors. Nonlinear processes such as these can be accommodated by the present analysis without seriously increasing the numerical effort. The only problem is to model the processes realistically.

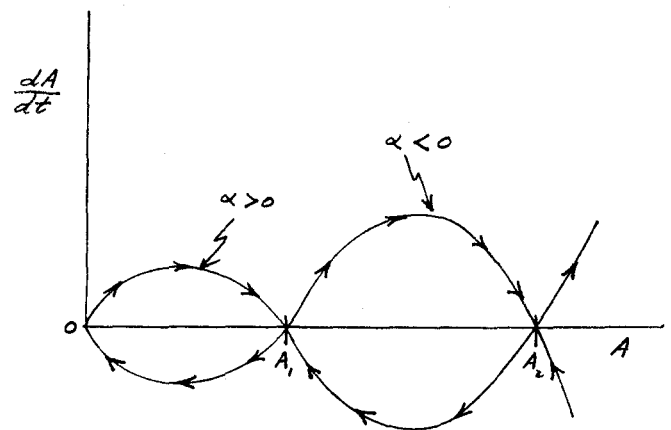


Fig. 5 Phase Plot for Equation (7.14).

### VIII. Combustion Coupling and Dynamics

At the present time there is widespread usage of only the simplest analysis of the influence of unsteady motions of the flow field on surface combustion<sup>(3)</sup>. The need for more comprehensive analytical work, and measurements, particularly of velocity coupling, is the most pressing in the entire subject of combustion instability.

Essentially, the problem is to determine the changes of velocity  $u_b'$  and mass flux  $m_b'$  of gases departing a burning surface in response to changes of the pressure and of the velocity parallel to the surface. By far most analytical work has been concerned with the response to pressure fluctuations (pressure coupling), and moreover, most calculations are founded on the following assumptions:

(i) Linearized motions, so that it is sufficient to treat harmonic disturbances. More general waveforms can be treated by superposition as, for example, in eqs. (6.5) and (6.6).

(ii) Heterogeneities are smeared out in some unspecified averaged way, so that the problem can be treated as one-dimensional in space.

(iii) Non-reacting solid phase. The conversion of solid to gas is supposed to occur at an infinitesimally thin interface according to some law, such as expressed by an Arrhenius rate law. What law is used has no influence on the form of the final result obtained for linear problems.

(iv) Quasi-steady behavior of the gas phase. This restricts the results to some range of "low" frequencies, but the upper limit is not known. The assumption can be justified mainly because the gas density is much less than the density of the solid. The range of validity is then reduced at higher operating pressures.

With these assumptions, all results for the response function  $R_b$  collapse to the single form independent of the model used for the flame structure in the gas phase:

$$R_b = \frac{\hat{m}_b / \bar{m}_b}{\hat{p} / \gamma \bar{p}} = \frac{\gamma [nAB + n_s(\lambda - 1)]}{\lambda + \frac{A}{\lambda} - (A+1) + AB} \quad (8.1)$$

The pressure index for the surface reaction is  $n_s$  and  $n$  is the index appearing in the law for the steady linear burning rate,  $\bar{F} \sim \bar{p}^n$ . This is a complex function of frequency through  $\lambda$ , which arises from the transient behavior of the thermal wave in the solid:  $\lambda(\lambda - 1) = i\Omega$ , where  $\Omega$  is the normalized angular frequency  $\Omega = \omega \kappa / \bar{F}^2$ .

Another complex function used to characterize linear transient behavior is the admittance function,  $A_b$ , which, for pressure coupling, is defined as

$$A_b = \frac{\hat{u}_b / \bar{a}}{\hat{p} / \gamma \bar{p}} \quad (8.2)$$

It is not difficult to show<sup>(11)</sup>, by use of the perfect gas law and the definition  $m_b = \rho u_b$ , that the non-isentropic temperature fluctuation at the edge of the combustion zone (see § III) is given in terms of  $R_b$  and  $A_b$  by the formula

$$\frac{\Delta \hat{T}}{\bar{T}_0} = [A_b + \bar{M}_b + \frac{1}{\gamma} (A_b + \bar{M}_b - \bar{M}_b R_b)] \frac{\hat{p}}{\gamma \bar{p}} \quad (8.3)$$

The definitions  $R_b$  and  $A_b$  can, of course, be

used in any linear analysis, and indeed, it is quite natural to introduce them as the discussions of §§ III and IV suggest. Similar functions can be defined for velocity coupling; but without further computations, such as those leading to the formula (8.1), or measurements, numerical values remain unknown.

Experiments to obtain  $R_b$  and  $A_b$  are very difficult to perform and are subject to considerable uncertainties. It is likely that the best one can hope for under any circumstances is that measured values will have uncertainties no greater than 10%. Virtually all experimental work has been done in T-burners. Some recent results with metallized propellants are discussed in refs. 8, 35-39, so the subject will not be covered in any detail here.

However, it should be noted that quite apart from the difficulties of minimizing experimental errors, the interpretation of data to obtain the desired numbers presents problems. The reason is that the T-burner is really just a peculiar form of rocket motor, so that the analyses discussed earlier must be used.\* Measured values of the growth constant  $\alpha$  are used with formulas such as (3.16) and (4.9) to deduce numerical values for whatever quantity is used to represent the combustion response. But for this procedure to work successfully, the remaining terms in the formula for  $\alpha$  must be known. See refs. 8 and 35 for a discussion of the effectiveness and limitations of the method.

Theoretical work on the combustion processes is necessary to understand the meaning of experimental results and is useful as an aid to formulating propellants. It is firmly established that the formula (8.1) does represent, in a qualitative way at least, the frequency response of unmetallized propellants. Therefore, there is little doubt that the transient conduction of heat within the solid phase is a dominant influence. Quantitative comparison with data leaves much to be desired<sup>(4)</sup>. It is fairly clear that calculations must be performed with one or more of the assumptions listed above relaxed. The following remarks cover briefly the present state of affairs. All of the works cited treat pressure coupling only.

Nonlinear calculations for practical purposes will, in all likelihood, be entirely numerical. In ref. 40, limited results were presented for the response to exponential changes of the impressed pressure. The gas phase was assumed to behave quasistatically; the computations involved mainly a finite difference solution to the nonlinear unsteady energy equation in a homogeneous non-reacting solid. This approach will probably also be used in a continuation of the work in ref. 18, but with more elaborate treatment of the gas phase. Analytical results for harmonic changes of pressure have been discussed in refs. 41-43, but the results become so complicated by a large number of parameters that it seems best to resort to a wholly numerical procedure. Some interesting results for very special cases have been reported in

\* That is, if the data are eventually to be incorporated in stability analysis of motors. But if the T-burner is used for comparing qualitatively the dynamical behavior of propellants, one is obviously much less concerned with precise results and very little analysis is necessary.

ref. 44; they are not suitable for stability analyses.

It is easy to see why nonlinear calculations are required. Realistic values of  $p'/\sqrt{\rho}$  can be as large as .2 - .3; values of the real part of  $R_b$  have been measured as large as 3 or so. Hence, the fluctuation  $m'_b/\bar{m}_b$  may be greater than .5, which is well outside the range one can reasonably expect linear analysis to be valid.

Most propellants used in practice are composites containing large mass fractions of solids, sometimes as large as 100  $\mu$  or more. Since the thermal wave has a characteristic length of the order of 10 - 50  $\mu$ , it is clear that the heterogeneous character of the material cannot be totally ignored. There are very few treatments of this problem, the most recent being refs. 45 and 46. Although some rather detailed conclusions are given, available experimental data are probably not sufficiently accurate to check them. The question has not been thoroughly studied. It appears that the most useful way of treating heterogeneities may be to determine the best method of averaging over the random properties of the material, and gas phase as well, to obtain a more tractable one-dimensional representation. This problem remains unsolved.

The influence of chemical reactions or decomposition in the solid phase has been examined by several workers<sup>(47-49)</sup>, but the results have thus far had little impact on the interpretation of data or on studies of stability. The recent work of ref. 48 deals with the influence of both chemical reactions in the solid phase and of oxidizer particle size. Very promising comparison of observations with the heuristic, semi-empirical analysis has been shown for both steady and unsteady burning. Reactions in the solid phase have long been a subject of study by Russian authors dealing principally with steady combustion of double-base propellants. Apart from one brief note<sup>(49)</sup>, the extension to unsteady burning has apparently not been done, and no work has been reported for composite propellants.

In ref. 50 a technique combining simple analysis and experimental data for steady-state combustion has been suggested for determining the transient properties of a burning solid. In principle, it accounts for heterogeneities and, possibly, but in a crude way, reactions in the solid. It does, however, rest crucially on the assumption of quasi-static behavior of the gas phase and requires experimental data not easily obtained to the precision necessary. The method amounts essentially to experimental determination of the parameters A and B in (8.1). Some success with the approach was reported.

The assumption of quasi-steady behavior merits examination, both because the frequencies of instabilities are often quite high, and because the approximation is less accurate at high pressures. Crude estimates in ref. 51 suggested that, indeed, there is basis for concern. Recently, some numerical results were reported<sup>(52)</sup> showing significant changes in the linear response function when the assumption is relaxed. No comparison with measurements has been attempted.

The two most important aspects of transient burning which have not been treated analytically in

any depth, are the influence of aluminum or other metal additives, and velocity coupling. The situation is essentially unchanged from that described in ref. 1.

### IX. Attenuation by Particulate Matter and the Solid Phase

The summary of the influence of particles given in ref. 1 still stands. Progress is slow, mainly because so little is known of the particles produced by a burning propellant. This problem is therefore intimately related to that of the combustion of aluminum, both near the propellant surface and farther out in the volume of the chamber. Two aspects of the theoretical behavior of inert particulate matter have been examined briefly.

In refs. 53 and 54 two detailed calculations for the attenuation by particles in rocket motors have been given. Well-known linear results<sup>(55, 56)</sup> for the behavior of a single particle have been used. The computations of ref. 53 provide numerical results for the damping of various modes with a non-uniform mean flow field. In ref. 54, a distribution of particle sizes is accounted for; the calculations show mainly slight shifts in the curves of attenuation vs. frequency. The changes are too small to be resolved within the data presently available from motor firings and T'-burner tests. Treatments based on average particle sizes therefore are adequate at the present time, although it does appear necessary to assume that two sizes are present. Experimental observations of burning aluminum drops have established beyond serious doubt that, in addition to the relatively small smoke particles, a considerable fraction of the mass is tied up in larger residual particles.

More interesting analytically is work on nonlinear behavior. Two works<sup>(57, 58)</sup> have dealt with this problem in essentially the same manner; preliminary results using a somewhat different analysis have been reported in ref. 59. The equation of motion for a single particle is solved assuming a nonlinear drag law. Then the time-averaged dissipation of energy is computed. In ref. 57, Oseen's drag law was used, but ref. 58 is based on an approximation to the measured drag on a spherical particle. Qualitatively, the results are similar: the absorption or attenuation coefficient increases with amplitude for relatively low frequencies. The upper limit depends on the particle size.

An important feature of particle attenuation is that there is an optimum particle size: for a given frequency, the attenuation has a maximum value as a function of particle radius. For typical conditions in a rocket motor, the optimum is in the vicinity of 8 - 10 microns at 800 Hz. The results of ref. 58 show that the attenuation increases for sizes greater than the optimum, and that the optimum value shifts to larger sizes as the amplitude of oscillation increases. But the maximum value of attenuation is essentially independent of amplitude.

Although it is not the purpose here to review experimental work, yet in connection with particulate damping, the recent work reported in refs. 60-62 must be mentioned. The results show very strikingly and indisputably the influence of certain compositional changes on the character of the agglomeration and combustion of aluminum near the surface of the propellant. Moreover, the ultimate

effect of those changes on the sizes of oxide particles produced, and hence on particulate damping of acoustic waves, was demonstrated qualitatively by data taken in T-burner firings.

The most thorough treatment of attenuation by the propellant grain appears in ref. 63. Several examples of application to full-scale motors are covered. Although the contribution to losses of acoustic energy may be significant, particularly in larger motors, there is considerable uncertainty in the values of material properties required in the calculations. Nevertheless, this is a part of the problem which deserved attention in any serious program devoted to combustion instability. Any results for practical configurations must be obtained numerically.

## X. Applications to Laboratory Devices and Motors

To the present time, application of the analyses discussed here has produced very spotty results. The best one can say is that there are examples for which qualitative behavior seems to have been correctly shown. There is no example of an accurate a priori prediction of a stability boundary for a motor. The main reason is the absence of experimental results, particularly for the response and admittance functions of the propellant. Computation of the attenuation of waves due to the presence of particles is also uncertain because the distribution and sizes of particles are not well known.

Apart from a few remarks concerning nonlinear behavior, the analysis of data taken in T-burners will not be discussed. The reader is referred to works already cited. In qualitative respects, much support for the approach outlined here has come from laboratory tests; indeed, certain observations have motivated the way in which the analysis has been developed. Linear behavior (in the sense that the amplitude of a wave grows or decays exponentially) is commonly seen in T-burners. The nonlinear growth to a limiting amplitude is, particularly with unmetallized propellants, likely to be influenced by processes which are less important in motors, such as heat transfer to inert walls. But data are relatively easily obtained, and repetitive firings can be done at considerably less expense than with motors. Hence, it is possible to make realistic checks of at least some parts of the analysis. What is learned from work with T-burners is for the most part directly applicable to motor problems, although this may not be immediately obvious.

It is well to begin with an enumeration of the information required to obtain numerical results for motors.

### (1) Classical Acoustic Modes and Frequencies

All of the formulas obtained here for the complex wavenumber - eqs. (3.14), (4.7), and (5.16) - and the nonlinear equation (7.3) for the amplitude, contain the unperturbed acoustic modes and corresponding wavenumbers. It is only in very simple cases, albeit important ones, that these functions can be easily represented analytically. For practical work with motors, by far the best procedure is to acquire this information numerically. For this purpose, the results of ref. 64, either as they are given there or in modified form, have proven very

useful. One dimensional and axisymmetric modes can be analyzed. General three-dimensional modes have not been studied, but these are much less important.

An alternative is to measure the mode structure and frequencies in scale models with no flow. A sonic exhaust nozzle must be treated as closed port with a rigid surface placed somewhere in the divergent section. The precise position depends on the nozzle, and can in principle be found independently by analysis or measurement<sup>(2)</sup>. However, an error in positioning the closure should have little influence on the acoustics information desired.

### (2) Transient Characteristics of the Nozzle

The nozzle admittance function can be either computed or measured. Recent work<sup>(2)</sup> has produced results for practical configurations when the flow is essentially room temperature air. There is no way of determining at the present time how the nozzle behaves when the flow consists of hot combustion gases containing particles. This is a very important problem, particularly if one is concerned with longitudinal modes. The nozzle then provides a major contribution to the losses of acoustic energy.

An interesting advantage afforded by the nozzle is that there is an opportunity to affect the stability of instabilities (at least if they are longitudinal modes, and perhaps otherwise) by relatively simple changes of geometry. It has been known since the earliest work on this subject that for a given entrance/throat area ratio, a shallow convergent section offers more attenuation than a steep section. This is not due to the projected area of the side walls, which depends only on the area ratio, but rather is due to the influence of gradients in the mean flow properties.

### (3) Influence of the Propellant Grain

Early work on this problem produced results in analytical form, although extremely complicated, for cylindrical configurations. For other cases, numerical calculations are required. It seems, however, that for practical purposes it is best always to use numerical methods, such as the finite-difference techniques of ref. 63. The absorption of energy by a grain varies widely with geometry, and hence during the firing of a motor. The major error appears to be due to the uncertainty in the values of propellant dynamical properties.

### (4) Propellant Response and Admittance Functions

Analysis of combustion coupling is useful at the present time mainly as an aid to correlating data. For application to motors, it is not necessary to have quantitative results, providing the appropriate measurements can be made. The quantities required for stability analysis, the real parts of (3.18) and (3.19), can in principle be extracted directly from data taken in T-burners, thereby eliminating the need for analysis.

Probably the most useful qualitative features of the response function (8.1) produced by analysis are that there is a peak; that the phase between the mass flux and pressure is positive at frequencies below the peak ( $m_b$  leads  $p'$ ) and negative above the peak ( $m_b$  lags  $p'$ ); and that the appropriate di-

dimensionless frequency is  $\Omega = \omega r / \sqrt{r^2}$ . For example, the peak for a given propellant occurs at a fixed value of  $\Omega$ . Hence, if the burning rate is increased the angular frequency  $\omega$  at which the peak occurs is also increased. This is perhaps the strongest effect of changing the operating pressure, but measurements suggest that the response curve itself shifts in ways not predicted by the analysis. For some propellants the response at a given value of  $\Omega$  increases with mean pressure, while for others it decreases; moreover, the shift is not in general uniform over the entire range of  $\Omega$ .

For a fixed geometry, the frequencies  $\omega$  of the modes are fixed. Consequently, if one has a rough idea of the shape of the response function, the influence of changing pressure can be assessed. Or, if the pressure is fixed, changes of geometry giving changes in the frequencies can be examined for their effects on stability by checking shifts along the response curve.

Measurements of pressure coupling for metallized propellants are difficult to take, mainly because the large losses associated with the particulate matter require either pulsed or extended area firings. The presence of the particles seems also to increase the errors in the data and harm reproducibility. But for velocity coupling, the situation is far worse: there is at the present time no satisfactory technique for acquiring the needed data. Under these circumstances, even a crude analysis would be helpful, particularly if the influence of aluminum could be represented.

There are difficulties in using T-burners, even with unmetallized propellants. They have been studied extensively and the most serious problems have been clearly delineated. In view of these difficulties, particularly the uncertainty of the influence of the vent<sup>(8, 35-39)</sup>, one might suppose that tests with small-scale motors would be more successful. Unfortunately, that is not true. The sonic exhaust nozzle presents its own problems; but the need for extended grains is the most serious difficulty, for it then becomes impossible to separate the effects of pressure and velocity coupling.

## (5) Other Contributions

Obviously, the mean flow field must be known, but this is easily obtained from the analyses of internal ballistics. The principal other contributions are the attenuation due to particles and the effects of residual combustion. They are not entirely disconnected, but at the present time, particulate damping is computed by using the results for inert particles. Until better information is available, there is little justification for doing otherwise. On the other hand, the problem of residual combustion should receive more attention than it has. Particularly in motors having low  $L^*$ , the coupling between burning far from the propellant surface and unsteady motions could conceivably be important.

### 10.1 Application to Laboratory Data

It appears that the best available data for checking the linear stability analysis are the observations reported in ref. 61. There are some difficulties in interpreting the results since the high-frequency instrumentation was not adequate to pro-

duce detailed records of the growths of unstable waves. However, the stability boundaries reported are probably good enough to check the validity of predictions. The influences of length, diameter, port/throat area ratio, and initial temperature were studied with cylindrical motors of unmetallized propellant (T-17).

In an attempt to compare analysis and observations, T-burner firings with the T-17 propellant were carried out in a later program<sup>(34, 66)</sup>. It seemed initially that satisfactory agreement had been obtained, but further work proved the contrary. Figure 6 shows the comparison finally obtained<sup>(34)</sup>. The predicted curve is computed from linear stability analysis with T-burner data used for the propellant admittance function.

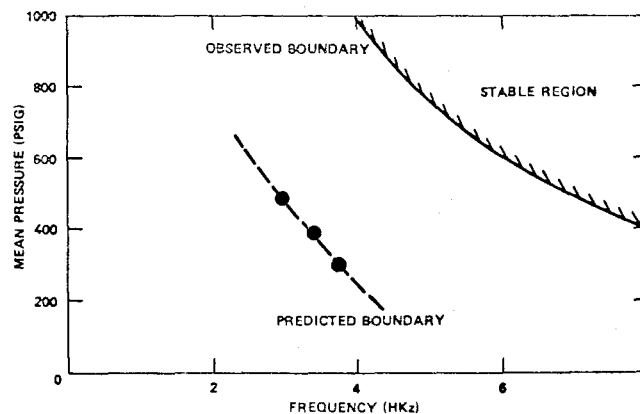


Fig. 6 Observed and Predicted Stability Boundaries for a Small Cylindrical Motor (refs. 34, 11).

There are several possible reasons for the poor agreement obvious in the figure. The unstable mode in this case is the lowest tangential mode having acoustic velocity components both parallel and normal to the surface: both  $\delta_{\parallel}$  and  $\delta_{\perp}$  defined in eq. (4.12) are non-zero. Hence, if the coupling is nonisentropic, then one must have data taken with both end and lateral grains, as the discussion of § III has shown. But the T-burner data used to construct the result shown in Fig. 10.1 were taken only with end grains. Consequently, the complete analysis of § III, which has been worked out since the experimental work shown in the figure, has not been checked. The formulas obtained for cylindrical ports<sup>(11)</sup> suggest that if the nonisentropic behavior is important, the theoretical boundary could be shifted significantly.

Experimental work is in progress at the Jet Propulsion Laboratory to obtain T-burner data for T-17 propellant with lateral grains. The results to date show both qualitative and quantitative differences between end and lateral burning configurations.

The interpretation of T-burner data is discussed at length in ref. 8. Here, only nonlinear behavior is briefly examined. It was, in fact, the relatively simple appearance of clean T-burner records which motivated the analysis given in ref. 31. Initial comparisons with T-burner records were very encouraging. Subsequent work based on eq. (7.14) has established that the growth to limiting amplitude is represented extremely well by the behavior of a nonlinear oscillator. Figure 10.2 is an example showing data and a numerical (by the method of least squares) fit of eq. (7.14).<sup>(67)</sup> The principal difficulty is that equally good fits can be obtained with rather broad ranges of the values of the parameters. Particular difficulties are encountered with data for metallized propellants. However, some progress has been made in identifying trends, and in certain cases the presence of nonlinear driving has been identified. A possible reason for the difficulties with this interpretation of the data is the presence of harmonics. Analysis of records which visually show no distortion indicates that in fact the amplitudes of higher harmonics may be as high as 10% of the fundamental. Hence, the question of harmonic coupling seems to be worth investigating.

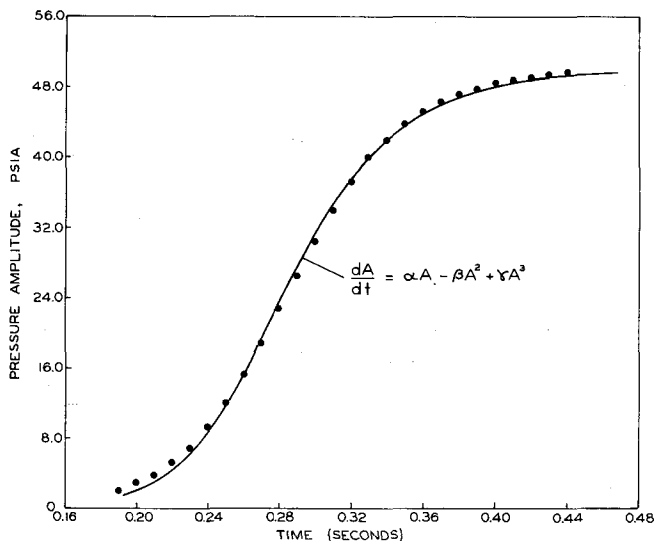


Fig. 7 Numerical Fit of Equation (7.14) to a T-Burner Pressure Record (ref. 66).

The value of this work is twofold: (1) to assess the validity of the approximate nonlinear analysis which, if favorable, can then be used to study motors; and (2) to gain quantitative information for the important nonlinear processes such as heat transfer, attenuation by particles, and combustion coupling. The importance to analysis of motors is obvious.

## 10.2 Application to Motors

Use of the linear stability analysis to study the transient behavior of motors consists in evaluating the various contributions to the expression (4.9) for the growth constant. The only case reported in published literature appears in ref. 68. The computations were based essentially on the analysis covered earlier in § IV except that the terms introduced from the one-dimensional analysis were not included.

Uncertainties in some of the input data were significant; for example, neither the response of the burning propellant nor the influence of the nozzle were known with great confidence; and the results were not in quantitative agreement with observations of motor behavior. The predicted growth rates decreased from several hundred ( $\text{sec}^{-1}$ ) at the beginning of a firing to values less than one hundred after 15 - 25 seconds. The oscillations in the motor were always found to decay after approximately 30 seconds. This comparison suggests that a trend in the behavior was correctly found, i. e., the driving decreases more rapidly than the damping with time; but the conclusion may be unfounded since the connection between linear growth rate and changes in the amplitude of oscillation is not clear.

The motor analyzed had 4 nozzles; initially the port consisted of a small center perforation with 4 slots. After a few seconds of burning the motor became an end burner. This configuration provided much structural damping by the propellant. In fact, nozzle, propellant, and particulate matter all contributed roughly the same attenuation, of the order of 60 - 80  $\text{sec}^{-1}$  initially. The driving by the propellant was computed to be in the range 300 - 400  $\text{sec}^{-1}$ , using data taken in T-burners.

Subsequent work<sup>(63)</sup> has shown that for a motor of size comparable to the one just cited, but having a full-length center bore, the attenuation by the propellant grain is smaller by a factor of 25 - 30; but for that motor, the driving was also much less, and the oscillations observed not only grew at smaller rates but attained considerably lower amplitudes. Full stability analysis of the motor also led to moderate qualitative success, but again,<sup>(69)</sup> serious uncertainties hampered the calculations.

In general, experiences with the linear stability analysis of motors seem to be similar to those described. The results often show correct trends, sometimes more strikingly than those quoted, but the known errors are too large for one to have confidence in the quantitative predictions.

Apart from the numerical calculations for small motors discussed in § VI, there are no nonlinear results available for motors.

An important practical question which has not been examined here is the use of suppression devices. Given that unstable motions may appear in a motor, and possibly when significant changes of design (geometry and propellant) cannot be made, one may have to find some other means of suppressing the oscillations or at least reducing the amplitude. What can be done depends very much on experience and testing. The action of suppression devices (acoustic liners, resonators, resonant rods or paddles, etc.) can be represented and accounted for in the analytical framework covered here. Some of

the necessary information, and discussions of particular examples may be found in ref. 69. It is sufficient here to note that the influence of a supersonic device on the basic acoustics (mode shape and frequency) of a chamber, as well as the coupling to the unstable modes, must be accounted for.

### XI. Concluding Remarks

It should be clear, particularly from the discussion of the preceding section, that the analysis of transient motions in combustion chambers must be evaluated in the context of both application to motors and interpretation of laboratory results. There are parts of the problem, mainly the behavior of the combustion processes and, to a lesser extent, the influence of the exhaust nozzle, which cannot be analyzed successfully from first principles. Experimental data are therefore essential to studying motors. On the other hand, analytical results are necessary for extracting the required information from small-scale laboratory experiments.

The uncertainties of measurements are such that it is not possible to state with complete confidence whether or not the analyses are correct or incomplete. At the present time the appropriate strategy seems to be to assume that the formal results are correct, with due allowance made for assumptions and approximations involved, and to use them until contrary evidence is found. The experiences so far have been such that unsatisfactory agreement between calculated predictions and observed behavior can generally be ascribed to inaccurate information required for quantitative results.

However, it is certainly true that the analyses summarized in this paper have been enormously helpful in making some sense of observations, for planning experimental work, and for producing at least qualitative predictions. So far as quantitative work is concerned, the situation may be summarized as follows.

The classical acoustics modes and frequencies required for all of the calculations discussed here can be obtained without great difficulty. Numerical computations are probably best, although measurements in a scale model (no flow) can also be used. All features of steady burning and flow in the chamber may also be assumed known.

By far the most serious problems arise in connection with the unsteady behavior of combustion and the nozzle. Recent work reported in ref. 2 eases the difficulties with the nozzle, but by no means entirely. The behavior with hot two-phase flows is simply not known. As emphasized several times, the interaction of waves with the nozzle constitutes a major contribution to the loss of acoustic energy for longitudinal modes in particular.

The greatest obstacle to successful predictions is the lack of a truly satisfactory means for studying the unsteady combustion of a burning propellant. Analyses of transient burning cannot alone produce the information needed for practical work. Much progress has been achieved with T-burners, but significant problems remain. The experiments are very difficult, and it appears that even under the best circumstances, one must expect errors of the order of 10%. Moreover, the test conditions in T-burners do not simulate in all respects the environment to which propellants are

exposed in motors. The most significant weakness is the lack of a technique for measuring velocity coupling.

There are other problems which need attention, but those mentioned are the most pressing at present. However, even though some of the crucial data may not be accurately known, much can be learned from analysis of a motor. It is possible, for example, to evaluate with considerable confidence the influence of grain geometry and flow field. And by a combination of experience and tests with T-burners (despite present difficulties) reasonable estimates can be made for the behavior of propellants. Hence, for practical purposes, one is generally in a position to make assessments of qualitative behavior, and of the consequences of possible changes in design.

### References

1. Culick, F. E. C., "Research on Combustion Instability and Application to Solid Propellant Rocket Motors," AIAA/SAE 7th Propulsion Joint Specialist Conference (June 1971), AIAA Paper No. 71-753.
2. Zinn, B. T., "Review of Present Understanding of Solid Propellant Rocket Motor Nozzles," AIAA/SAE 8th Propulsion Joint Specialist Conference (Nov. 1972).
3. Culick, F. E. C., "A Review of Calculations for Unsteady Burning of a Solid Propellant," AIAA J., V. 6, no. 12 (Dec. 1968), pp. 2241-2255.
4. Beckstead, M. W. and Culick, F. E. C., "A Comparison of Analysis and Experiment for Solid-Propellant Combustion Instability," AIAA J., V. 9, no. 1 (Jan. 1971), pp. 147-154.
5. Price, E. W., "Experimental Solid Propellant Rocket Combustion Instability," Tenth Symposium (International) on Combustion, The Combustion Institute, Pittsburgh, Pa. (1965), pp. 1067-
6. Price, E. W., "Recent Advances in Solid Propellant Combustion Instability," Twelfth Symposium (International) on Combustion, The Combustion Institute, Pittsburgh, Pa., (1969), pp. 101-113.
7. Price, E. W., Mathes, H. B., Madden, O. H., and Brown, B. G., "Pulsed T-Burner Testing of Combustion Dynamics of Aluminized Solid Propellants," AIAA/SAE 7th Joint Propulsion Specialist Conference (June 1971), AIAA Paper 71-
8. Andrepont, W. C. and Schoner, R. J., "The T-Burner Test Method for Determining the Combustion Response of Solid Propellants," AIAA/SAE 8th Propulsion Joint Specialist Conference (Nov. 1972).
9. Roberts, A. K. and Brownlee, W. G., "Non-linear Combustion Instability: the Influence of Propellant Composition," AIAA J., V. 9, no. 1 (Jan. 1970), pp. 140-147.

10. Marble, F. E. , "The Dynamics of Dusty Gases," Ann. Rev. of Fl. Mech., V.2 (1970) pp. 397-446.
11. Culick, F. E. C. , "Interactions Between the Flow Field, Combustion, and Wave Motions in Rocket Motors," Naval Weapons Center, China Lake, Calif., NWC TP 5349 (June 1972).
12. McClure, F. T. , Hart, R. W. , and Bird, J. F. , "Solid Propellant Motors as Acoustic Oscillators," Progress in Astronautics and Rocketry, V.1, Academic Press (1960), pp. 295-358.
13. Hart, R. W. and McClure, F. T. , "Theory of Acoustic Instability in Solid-Propellant Rocket Combustion," Tenth Symposium (International) on Combustion, The Combustion Institute, Pittsburgh, Pa. (1965), pp. 1047-1065.
14. Cantrell, R. H. and Hart, R. , "Interaction between Sound and Flow in Acoustic Cavities; Mass Momentum and Energy Considerations," J. Acoust. Soc. Amer., V. 36, no. 4 (April 1964), pp. 697-706.
15. Culick, F. E. C. , "Acoustic Oscillations in Solid Propellant Rocket Chambers," Astronautica Acta, V. 12, no. 2 (1966), pp. 114-126.
16. Flandro, G. A. , "Rotating Flows in Acoustically Unstable Rocket Motors," Ph. D. Thesis, California Institute of Technology (Mar. 1967).
17. Morse, P. M. and Feshbach, H. , Methods of Theoretical Physics, McGraw-Hill Book Co. , New York (1953).
18. Levine, J. N. and Culick, F. E. C. , "Numerical Analysis of Nonlinear Longitudinal Combustion Instability in Metallized Propellant Solid Rocket Motors," Ultrasystems, Inc. (formerly Dynamic Science), July 1972. Air Force Rocket Propulsion Laboratory Report TR 72-88.
19. Micheli, P. L. , Aerojet Solid Propulsion Co. , Sacramento, Calif. (private communication).
20. Hart, R. W. , Bird, J. F. , and McClure, F. T. , "The Influence of Erosive Burning on Acoustic Instability in Solid Propellant Rocket Motors," Progress in Astronautics and Rocketry, V.1, Academic Press (1960), pp. 295-358.
21. McClure, F. T. , Bird, J. F. , and Hart, R. W. , "Erosion Mechanism for Nonlinear Instability in Axial Modes of Solid Propellant Rocket Motors," ARS J., V. 32, no. 3 (Mar. 1962), pp. 374-378.
22. Price, E. W. and Dehority, G. L. , "Velocity Coupled Axial Mode Combustion Instability in Solid Propellant Rocket Motors," ICRPG/AIAA 2nd Solid Propulsion Conference (June 1967), pp. 213-227.
23. Culick, F. E. C. , "Stability of Longitudinal Oscillations with Pressure and Velocity Coupling in a Solid Propellant Rocket," Combustion Science and Technology, V. 2, no. 4 (Dec. 1970), pp. 179-201.
24. Epstein, P. S. and Carhart, R. R. , "The Absorption of Sound in Suspensions and Emulsions," J. Acoust. Soc. Amer., V. 25, no. 3 (Mar. 1953), pp. 553-565.
25. Temkin, S. and Dobbins, R. A. , "Attenuation and Dispersion of Sound by Particulate-Relaxation Processes," J. Acoust. Soc. Amer., V. 40, no. 2 (Feb. 1966), pp. 317-324.
26. Dehority, G. L. , "A Parametric Study of Particulate Damping Based on the Model of Temkin and Dobbins," Naval Weapons Center, China Lake, Calif. (Sept. 1970), NWC TP 5002.
27. Culick, F. E. C. , "Nonlinear Behavior of Acoustic Waves in Combustion Chambers," supported by Hercules, Inc., Magna, Utah.
28. Zinn, B. T. and Powell, E. A. , "Nonlinear Combustion Instability in Liquid-Propellant Rocket Engines," Thirteenth Symposium (International) on Combustion, The Combustion Institute, Pittsburgh, Pa. (1970), pp. 491-504.
29. Zinn, B. T. and Powell, E. A. , "A Single Mode Approximation in the Solution of Nonlinear Combustion Instability Problems," Combustion Science and Technology, V. 3 (1971), pp. 121-132.
30. Zinn, B. T. and Lores, M. E. , "Application of the Galerkin Method in the Solution of Nonlinear Axial Combustion Instability Problems in Liquid Rockets," Combustion Science and Technology, V. 4 (1972), pp. 269-278.
31. Culick, F. E. C. , "Nonlinear Growth and Limiting Amplitude of Acoustic Oscillations in Combustion Chambers," Combustion Science and Technology, V. 3 (1971), pp. 1-16.
32. Krylov, N. and Bogoliubov, N. , Introduction to Nonlinear Mechanics, Princeton University Press, Princeton, N. J. (1947).
33. Kevorkian, J. , "The Two Variable Expansion Procedure for the Approximate Solution of Certain Nonlinear Differential Equations," in Lectures in Applied Mathematics, V. 7, Space Mathematics, Part III, Amer. Math. Soc. (1966), pp. 206-275.
34. Perry, E. H. , "Investigation of the T-Burner and Its Role in Combustion Instability Studies," Ph. D. Thesis, California Institute of Technology, Pasadena, Calif. (June 1970).
35. Derr, R. L. , Price, C. F. , and Culick, F. E. C. , "Analysis of T-Burner Data Obtained by AFRPL Workshop Participants for a Metallized Propellant (ANB-3066)," 9th JANNAF Combustion Meeting (Sept. 1971).
36. Peterson, J. A. , Presentation at a Panel Discussion on the Use of T-Burners, 9th JANNAF Combustion Meeting (Sept. 1971).

37. Beckstead, M. W., Ibid.
38. Micheli, P. L., Ibid.
39. Price, E. W., Ibid.
40. Krier, H., Tien, J. S., Sirignano, W. A., and Summerfield, M., "Nonsteady Burning Phenomena of Solid Propellants: Theory and Experiments," AIAA J., V. 6, no. 2 (Feb. 1968), pp. 178-185.
41. Friedly, J. C. and Peterson, E. E., "Influence of Combustion Parameters on Instability in Solid Propellant Motors; Part II. Nonlinear Analysis," AIAA J., V. 4, no. 7 (July 1966), pp. 1932-1937.
42. Brown, R. S. and Muzzy, R. J., "Linear and Nonlinear Pressure Coupled Combustion Instability of Solid Propellants," AIAA J., V. 8, no. 8 (Aug. 1970), pp. 1492-1500.
43. Novozhilov, B. V., "Nonlinear Oscillations of Combustion Velocity of Powder," J. Appl. Mech. and Tech. Physics, V. 7, no. 5 (1966), pp. 31-41.
44. Librovich, V. B. and Novozhilov, B. V., "Self-Similar Solutions in the Nonsteady Propellant Burning Rate Theory and Their Stability Analysis," Combustion Science and Technology, V. 4, no. 6 (Feb. 1972), pp. 257-268.
45. Law, C. K. and Williams, F. A., "Some Theoretical Aspects of the Influence of Solid Heterogeneity on L\* Instability," AIAA 10th Aerospace Sciences Meeting, San Diego, Calif. (Jan. 1972), AIAA Paper No. 72-33.
46. Williams, F. A. and Lengelle, G., "Simplified Model for Effect of Solid Heterogeneity on Oscillatory Combustion," Astronautica Acta, V. 14 (1969), pp. 97-118.
47. Culick, F. E. C., "Calculation of the Admittance Function for a Burning Surface," Astronautica Acta, V. 13 (1967), pp. 221-237.
48. Kumar, R. N., "Some Considerations in the Combustion of AP/Composite Propellants," Guggenheim Jet Propulsion Center, California Institute of Technology (Aug. 1972).
49. Novozhilov, B. V., "Stability Criterion for Steady-State Burning of Powders," J. Appl. Mech. and Tech. Physics, V. 4 (July/Aug. 1965), pp. 157-160.
50. Summerfield, M., et al., "Theory of Dynamic Extinguishment of Solid Propellants with Special Reference to Nonsteady Heat Feedback Law," J. Spacecraft and Rockets, V. 8, no. 3 (Mar. 1971), pp. 251-258.
51. Culick, F. E. C., "Some Problems in the Unsteady Burning of Solid Propellants," Naval Weapons Center, China Lake, Calif. (Feb. 1969), NWC TP 4668.
52. Tien, J. S., "Oscillatory Burning of Solid Propellants Including Gas Phase Time Lag," Combustion Science and Technology, V. 5, no. 2 (April 1972), pp. 47-54.
53. Yang, J. Y. S., "Particulate Damping in Solid Propellant Rockets," AIAA J., V. 10, no. 3 (Mar. 1972), pp. 337-338.
54. Hopkins, B. D. and Krashin, M., "Damping of Small Amplitude Acoustic Waves by Non-Burning Particles in T-Burners and Rocket Motors," AIAA/SAE 7th Propulsion Joint Specialist Conference (June 1971), AIAA Paper No. 71-633.
55. Epstein, P. S. and Carhart, R. R., Ibid.
56. Temkin, S. and Dobbins, R. A., Ibid.
57. Mednikov, E. P., "Absorption and Dispersion of Sound in Aerosols at Large Particle Velocity Amplitudes," Soviet Physics-Acoustics, V. 15, no. 4 (April/June 1970), pp. 507-510.
58. Korman, H. F. and Michele, P. L., "Nonlinear Particulate Damping of Acoustic Oscillations," 8th JANNAF Combustion Meeting, Vol. 1, C. P. I. A. Publication 220 (Nov. 1971), pp. 345-550.
59. Jensen, R. C., "Particulate Damping of Acoustic Waves - Nonlinear Effects," 9th JANNAF Combustion Meeting (Sept. 1972).
60. Kraeutle, K. J., "The Behavior of Aluminum During Sub-Ignition Heating and Its Dependence on Environmental Conditions and Particle Properties," 9th JANNAF Combustion Meeting (Sept. 1972).
61. Boggs, T. L., Kraeutle, K. J., and Zurn, D. E., "Combustion of As-received and Pre-oxidized Aluminum in Sandwich and Propellant Configurations," 9th JANNAF Combustion Meeting (Sept. 1972).
62. Price, E. W., Mathes, H. B., and Kraeutle, K. J., "Effect of Partial Preoxidation of Aluminum on Oscillatory Combustion Behavior of an HTPB-AP Propellant," 9th JANNAF Combustion Meeting (Sept. 1972).
63. Anderson, J. Mc., "Structural Damping of Acoustic Oscillations in Solid Propellant Rocket Motors," 8th JANNAF Combustion Meeting, C. P. I. A. Publication 220 (Nov. 1971), pp. 321-343.
64. Herting, D. N., et al., "Acoustic Analysis of Solid Rocket Motor Cavities by a Finite Element Method," McNeal-Schwendler Corp., Los Angeles, Calif. (Aug. 1971), AFRPL-TR 71-96.
65. Brownlee, W. G. and Marble, F. E., "An Experimental Investigation of Unstable Combustion in Solid Propellant Rocket Motors," in Progress in Astronautics and Rocketry, V. 1, Academic Press, New York (1960), pp. 455-494.
66. Beckstead, M. W., Hercules, Inc. (private communication).
67. Browning, S. C., Krashin, M., and Thasher, J. H., "Application of Combustion Instability

Technology to Solid-Propellant Rocket Motor Problems," AIAA/SAE 7th Propulsion Joint Specialist Conference (June 1971), AIAA Paper No. 71-754.

69. Oberg, C. L., Wong, T. L., and Haymes, W.G., "Solid Propellant Combustion Instability Suppression Devices," AIAA/SAE 8th Propulsion Joint Specialist Conference (Nov. 1972).